

Terrain-Induced Rotor Experiment

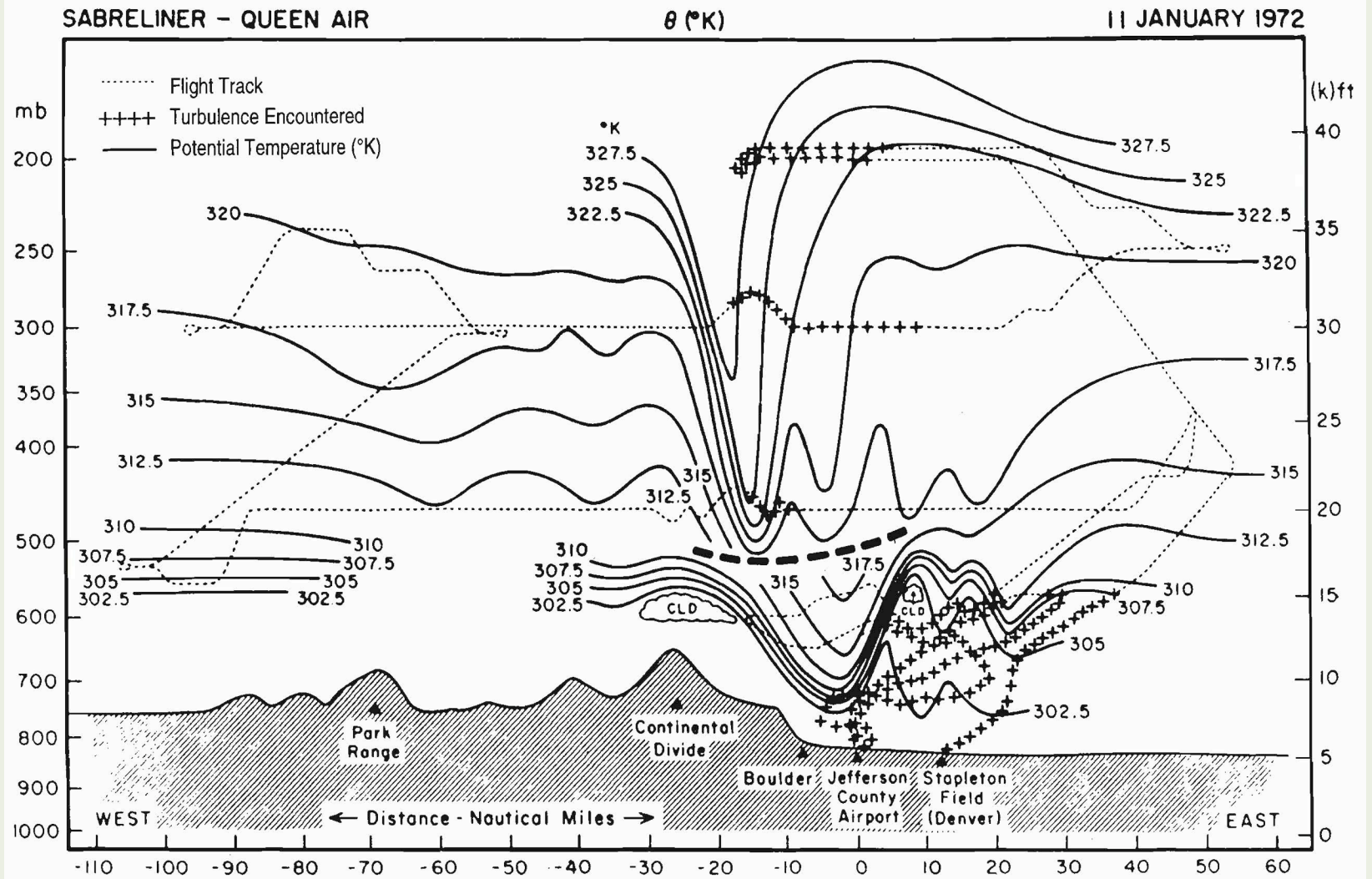


Wave-induced Turbulence in the Lower Troposphere: A T-REX Perspective

Vanda Grubišić

Division of Atmospheric Sciences
Desert Research Institute

Acknowledgements: June Wang (NCAR), Lakshmi Kantha (CU Boulder),
James Doyle (NRL Monterey), Qinfang Jiang (NRL Monterey),
Al Rodi (U Wyoming)



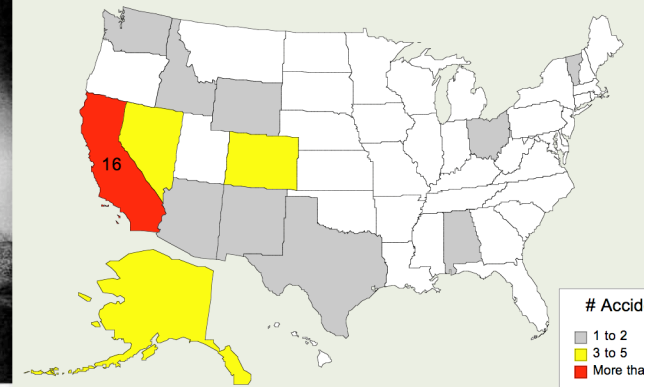
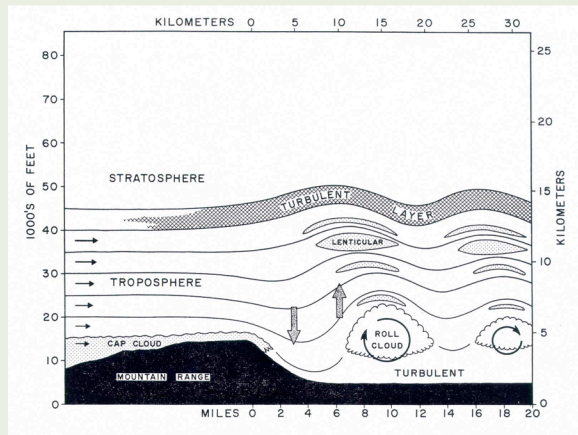
Lilly (1978)

Outline

- Background on atmospheric rotors
- Terrain-induced Rotor Experiment (T-REX)
- Turbulence structures from aircraft data
- Turbulence from radiosonde data
- Summary

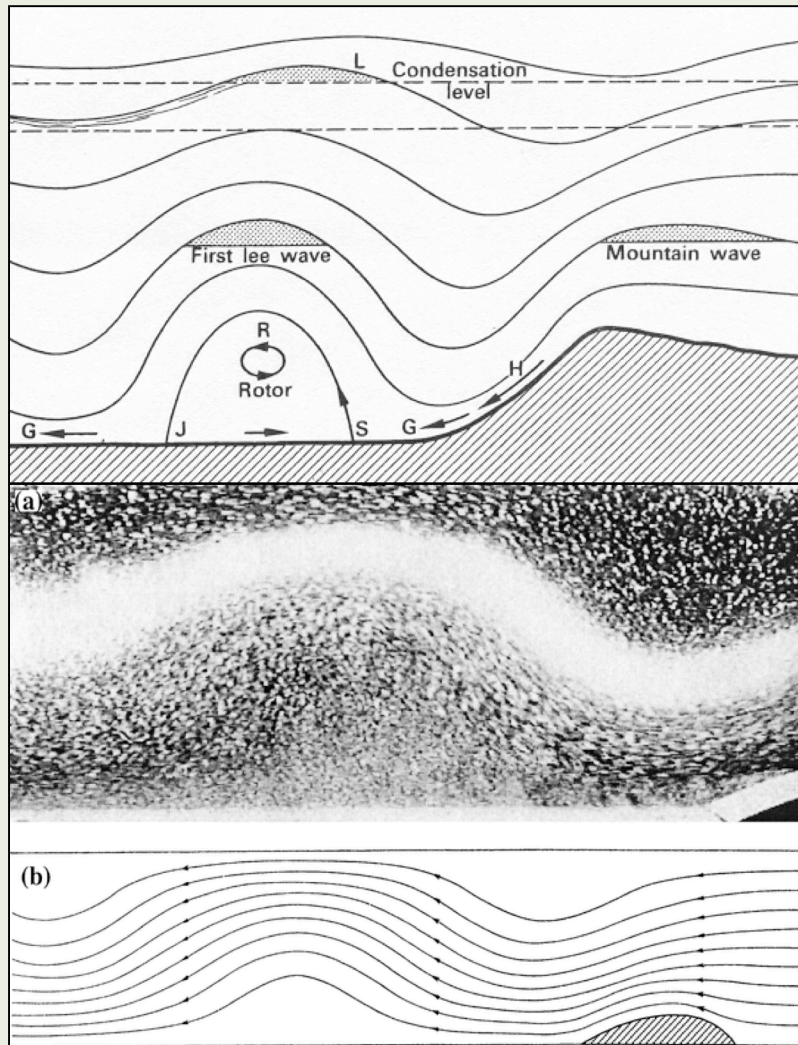
Atmospheric Rotors

Mountain Wave Induced Turbulence at Lower Tropospheric Levels



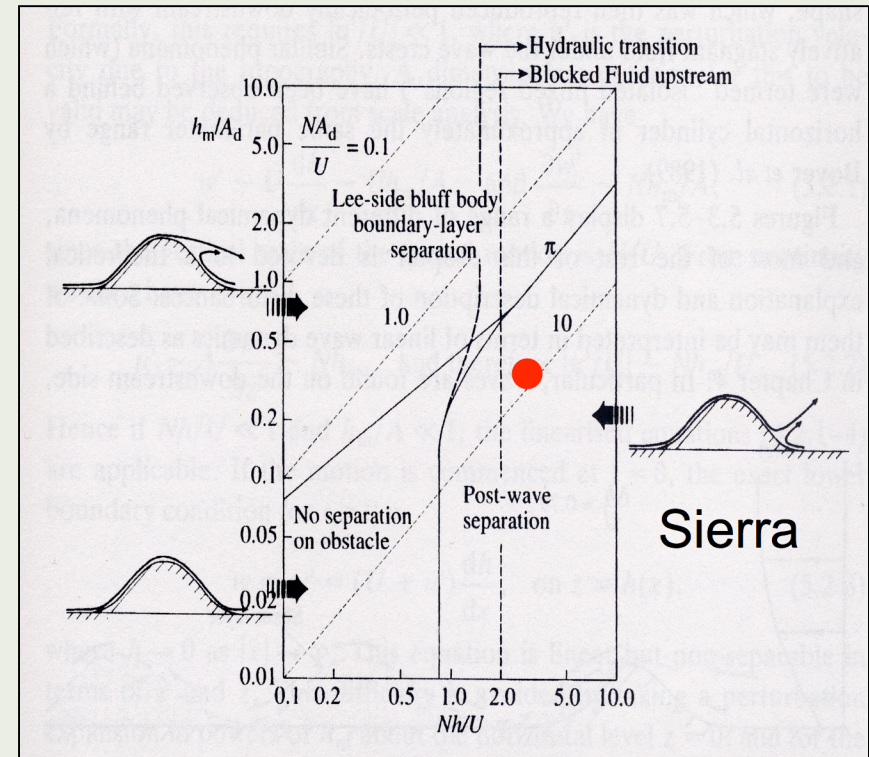
- Forming a strongly coupled system with overlying mountain waves and underlying boundary layer
- Improved understanding and prediction important for aviation safety in complex terrain

Rotor Origin: Wave-induced BL Separation



Long (1955)

March 29, 2008



Baines (1995); Baines & Hoinka (1985)

Recent idealized numerical studies:

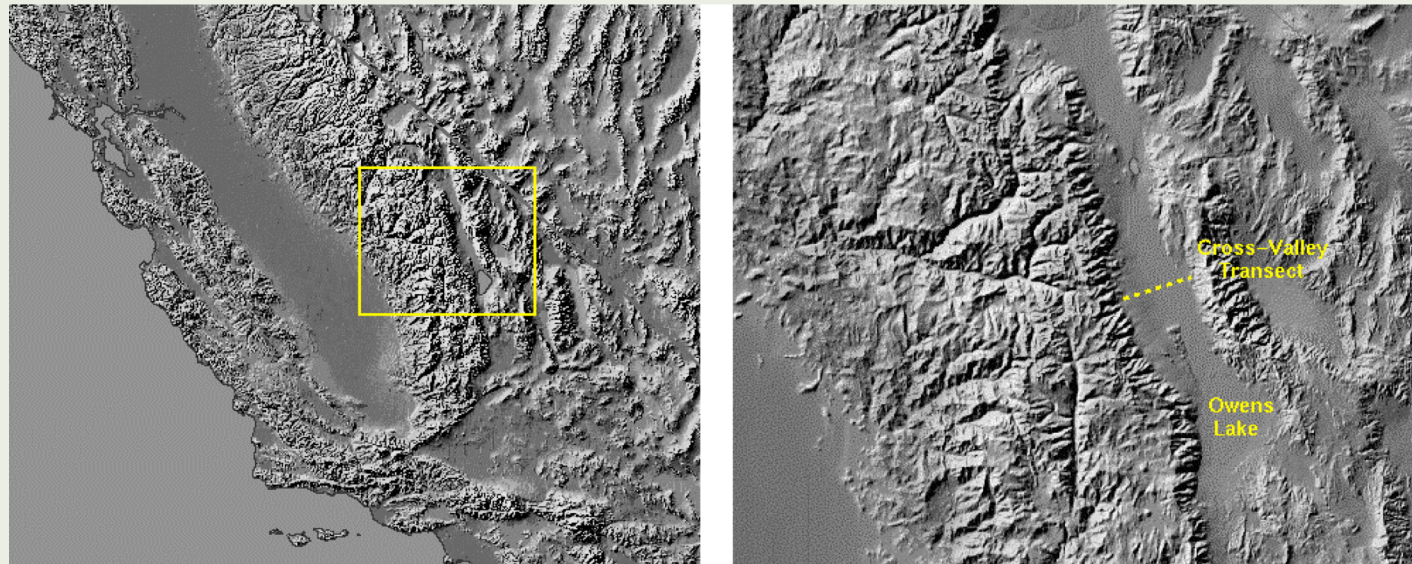
- | | |
|-------------------------|----|
| Doyle and Durran (2002) | 2D |
| Vosper et al. (2006) | 2D |
| Jiang et al. (2007) | 2D |
| Doyle and Durran (2007) | 3D |

Field Campaign

Phase I **Sierra Rotors**
Mar-Apr 2004

Phase II **T-REX**
Mar-Apr 2006

Field site of both phases
Southern Sierra Nevada Eastern California

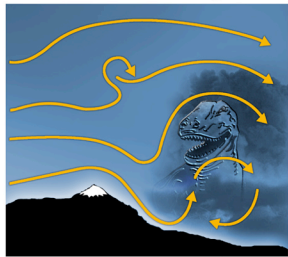


May 29, 2008

IMAGe TOY 2008 Geophysical
Turbulence Phenomena

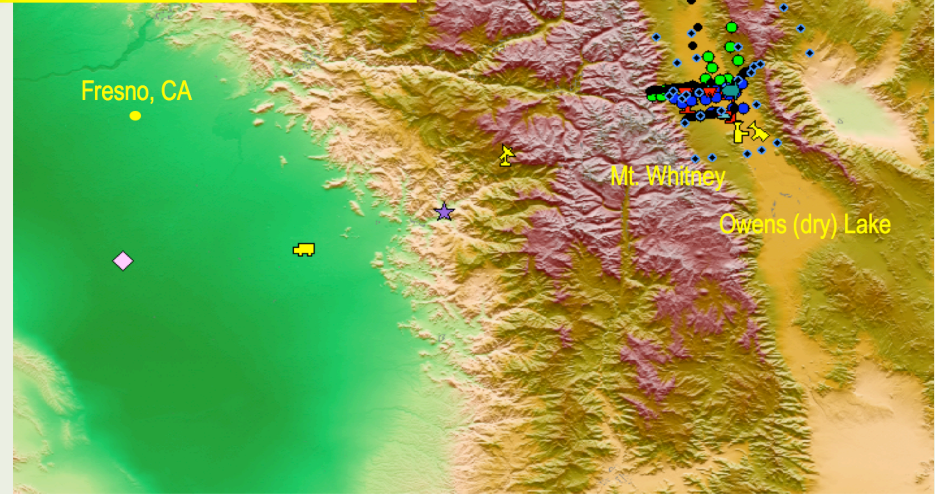
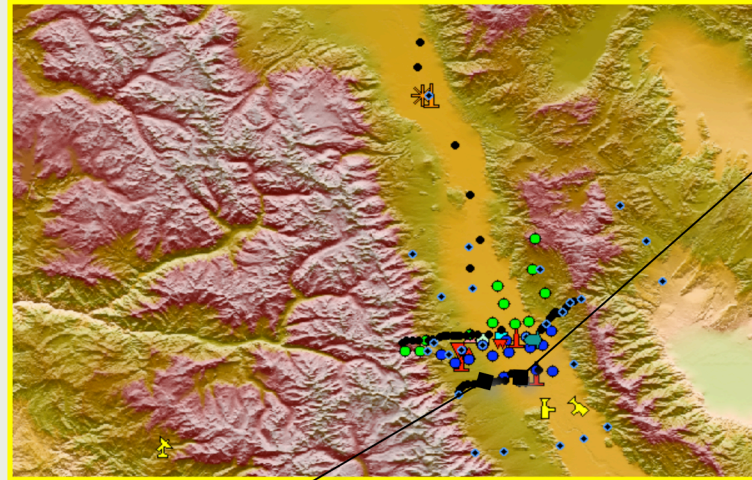
6

Terrain-Induced Rotor Experiment



T-REX Experiment Design Ground-based Instrumentation

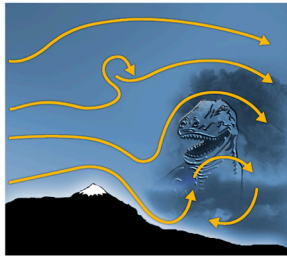
- Yale video cameras
- CU Tethered Lifting System
- Yale K-band Radar
- NCAR Soil M&T
- U. Innsbruck instrumented car
- NCAR MISS
- NCAR ISS DBS
- NCAR ISS MAPR
- AFRL Thermosonde
- GPS sounding site
- MGLASS
- U. Utah HOBOS
- DRI AMS
- U. Leeds AMS
- U. Houston flux tower
- U. Houston sodar
- NRL Aerosol Lidar
- NCAR REAL
- ASU Doppler Lidar
- DLR Doppler Lidar
- NCAR ISFF



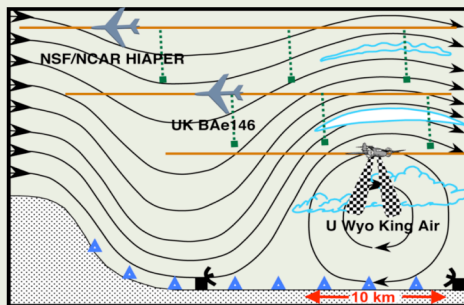
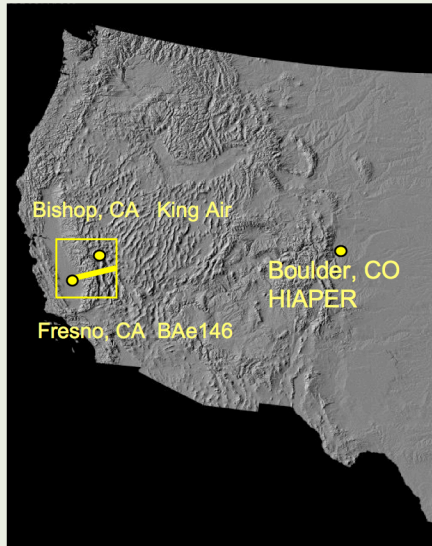
May 29, 2008

IMAGE TOY 2008 Geophysical
Turbulence Phenomena

Terrain-Induced Rotor Experiment



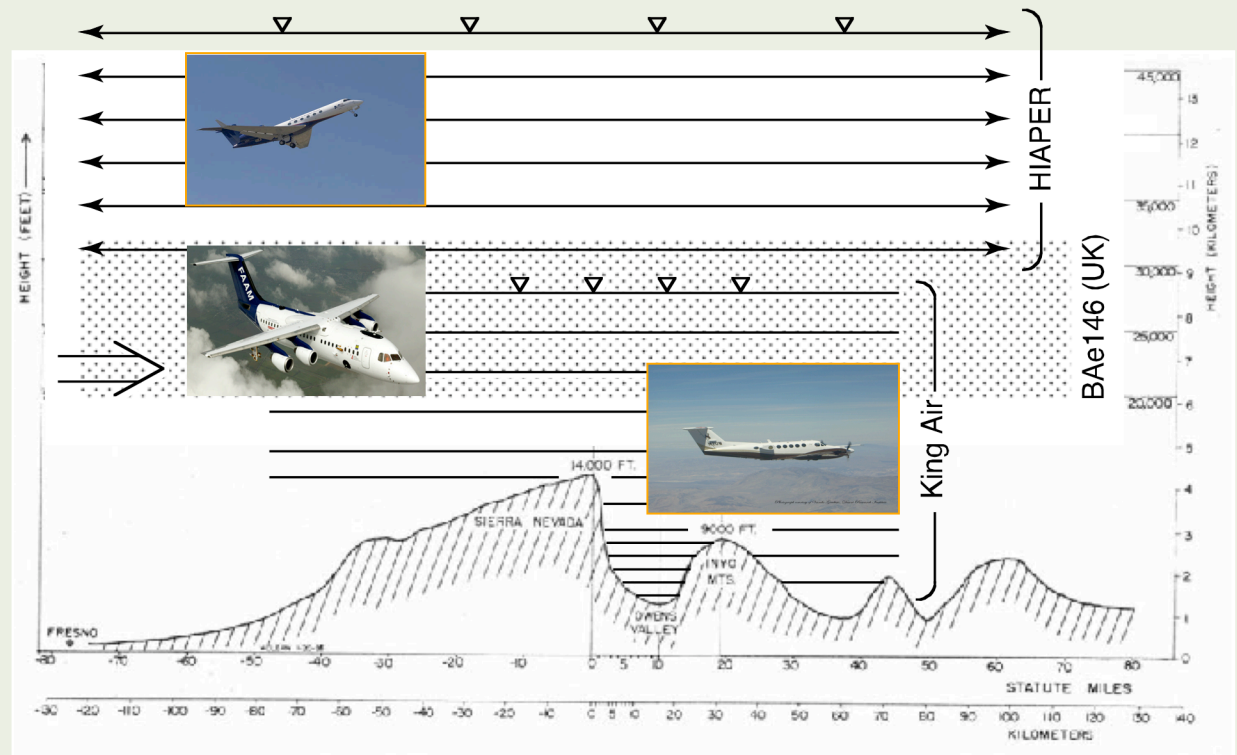
T-REX Experiment Design Airborne Platforms



- ground-based lidars
- jet aircraft
- surface stations
- turbo-prop aircraft with cloud radar
- dropsondes



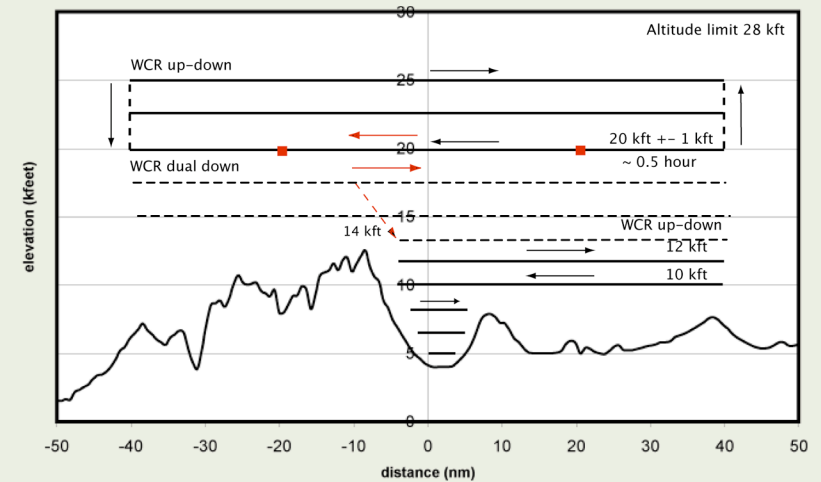
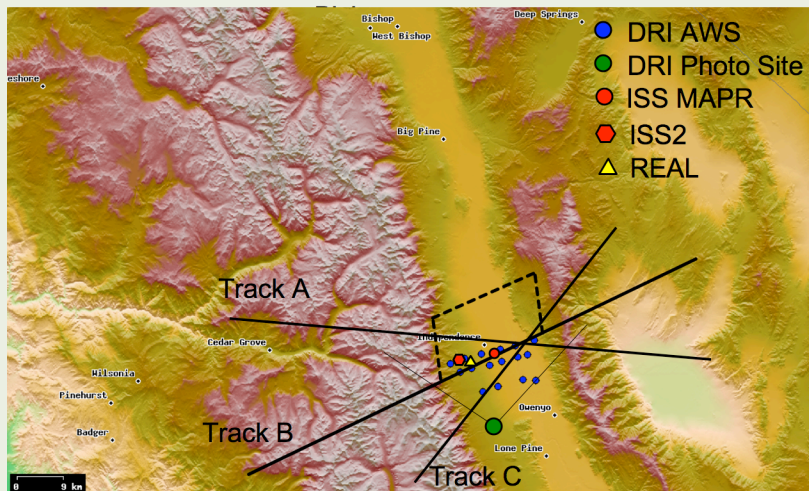
▽ Dropsondes



May 29, 2008

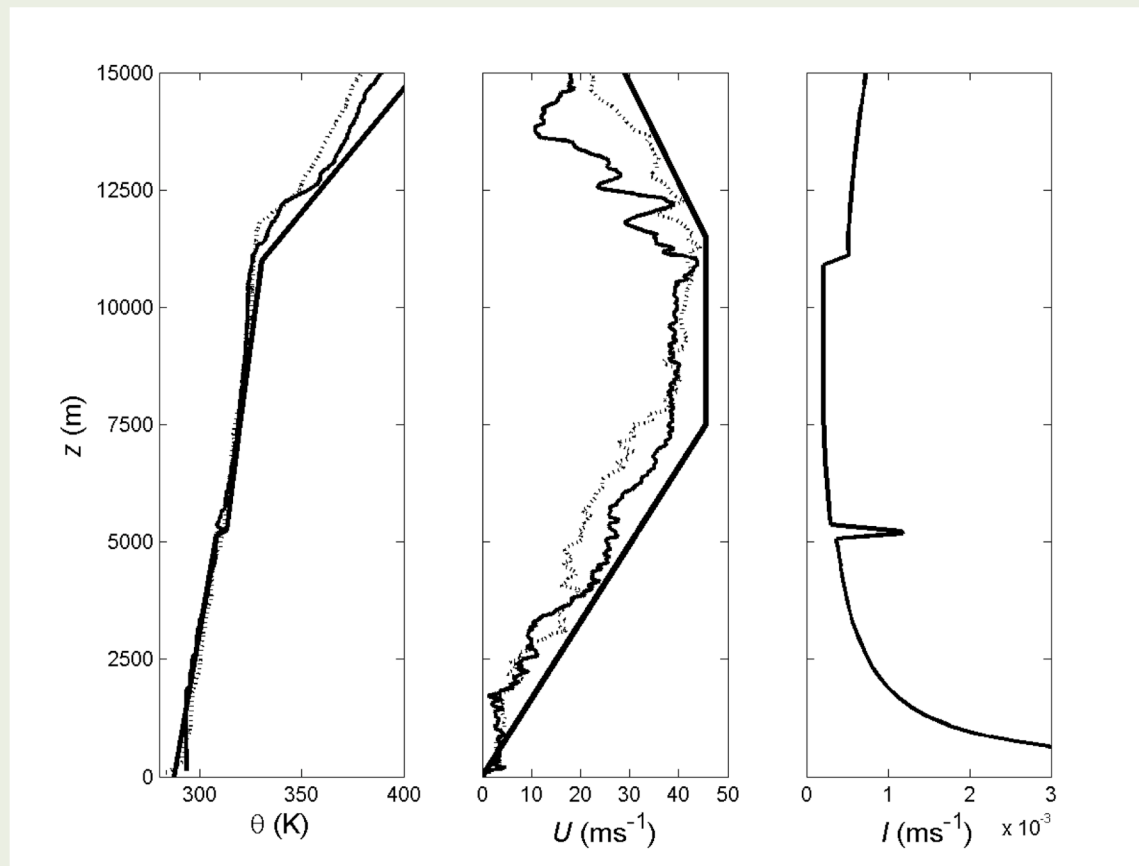
IMAGE TOY 2008 Geophysical
Turbulence Phenomena

King Air Missions in T-REX



- 25 research flights
- Average duration 3.5 hrs
- Only 3 single UWKA research flights (IOP 5, IOP 11, IOP 12)
- Only 2 research flights flown outside the target area (IOP 15)
- Basic cross-mountain tracks: A (275°), B(245°), C(215°)
- Vertical stack and box

Typical Upstream Profile



$$N \sim 0.01 \text{ s}^{-1}$$

$$U \sim 15\text{-}20 \text{ ms}^{-1}$$

$$H \sim 3 \times 10^3 \text{ m}$$

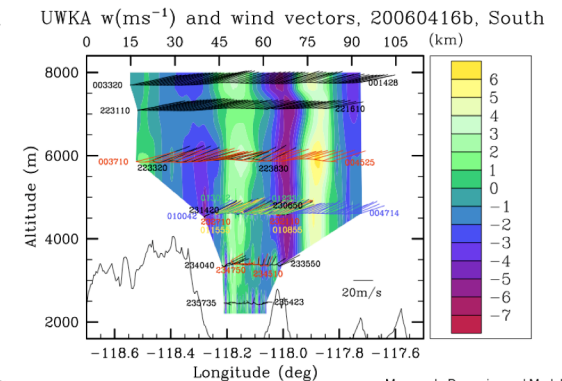
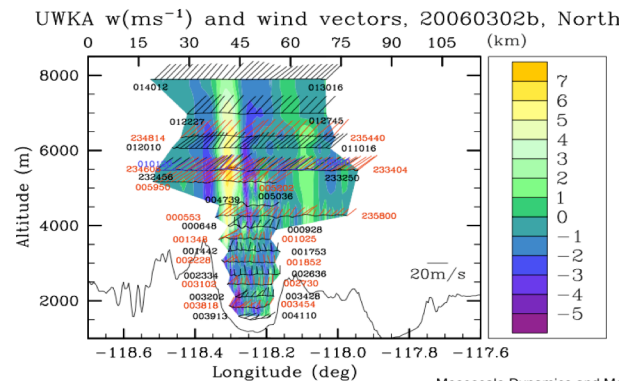
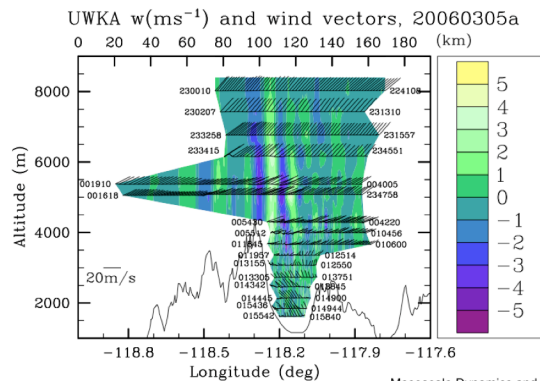
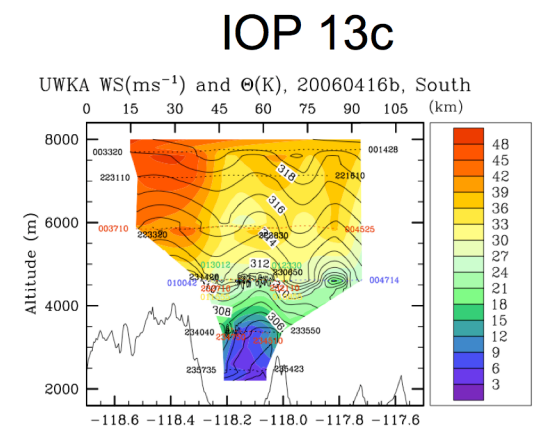
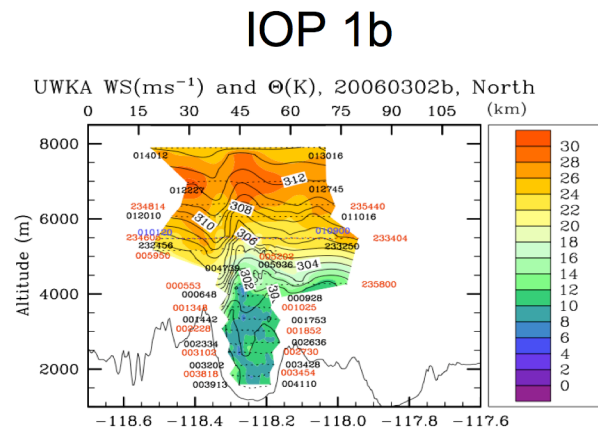
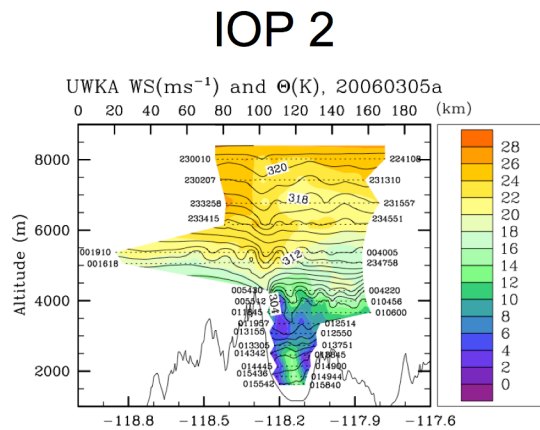
$$\text{Fr} = U/NH \sim 0.5\text{-}0.7$$

May 29, 2008

IMAGe TOY 2008 Geophysical
Turbulence Phenomena

10

Observed Lower-Tropospheric Wave Structures Moderate → Large Amplitude

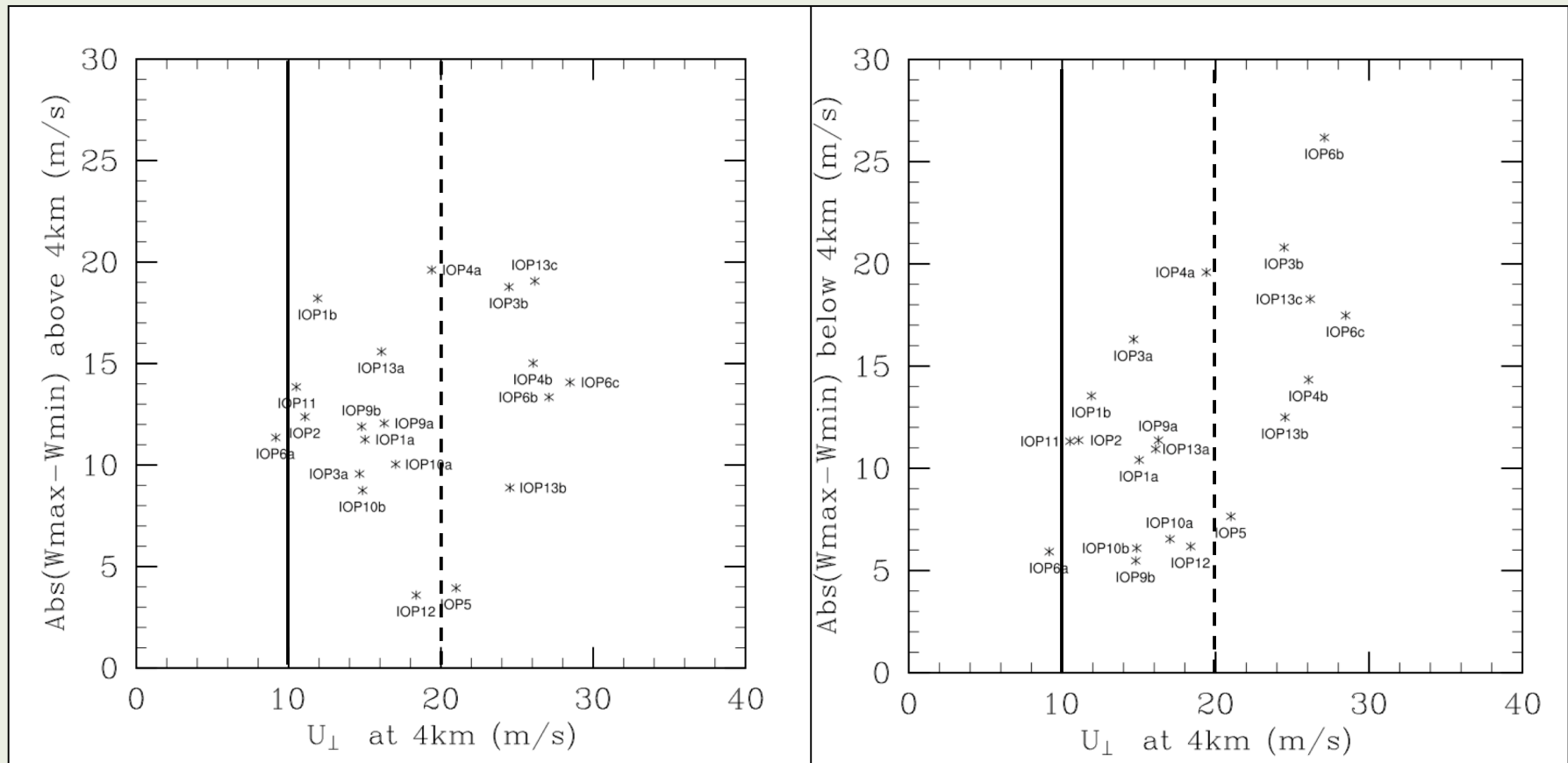


Mesoscale Dynamics and Modeling
Vanda.Grubicic@dri.edu

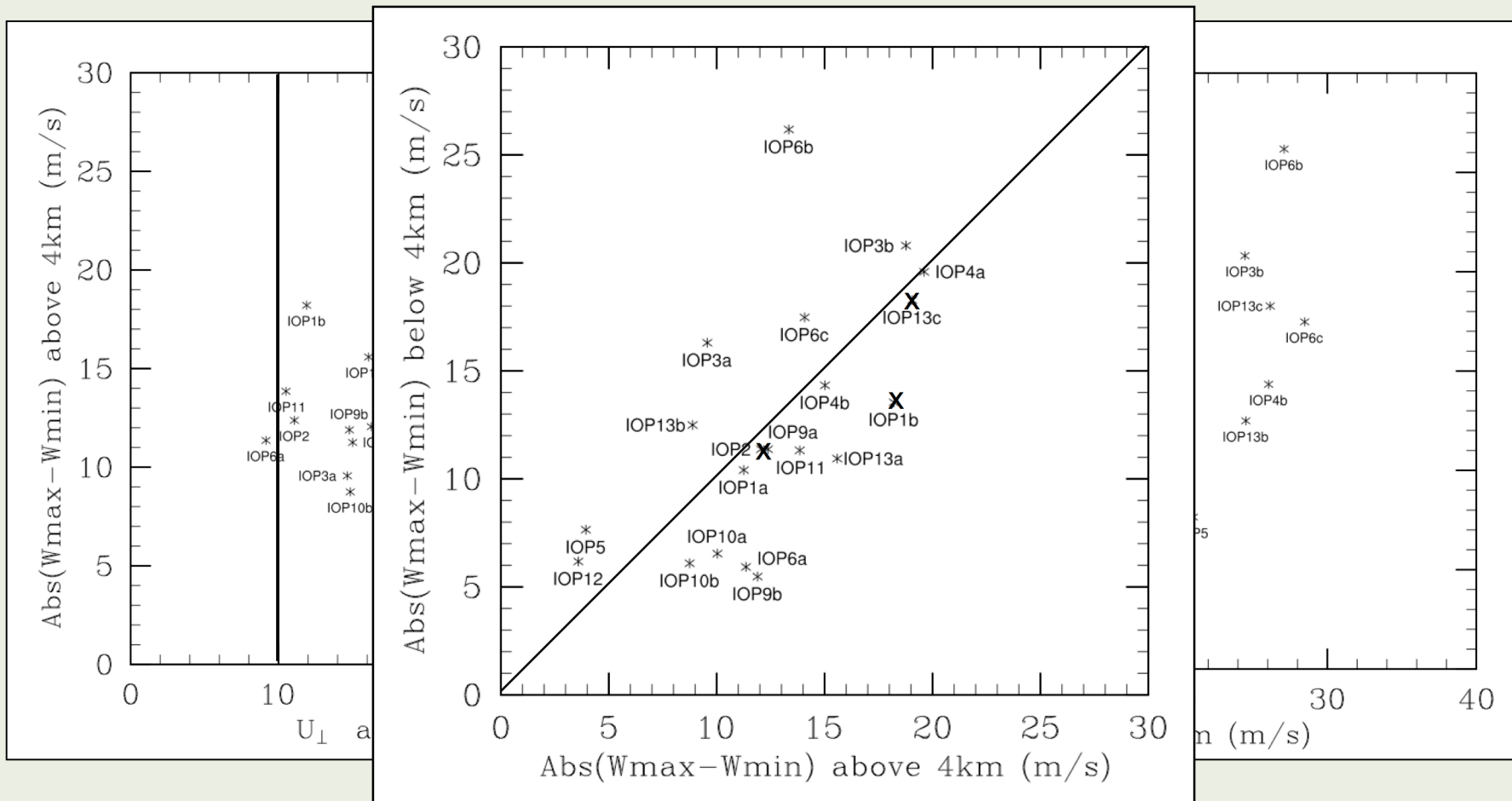
Mesoscale Dynamics and Modeling
Vanda.Grubicic@dri.edu

Mesoscale Dynamics and Modeling Labora
Vanda.Grubicic@dri.edu

All Flights 1Hz Data



All Flights 1Hz Data

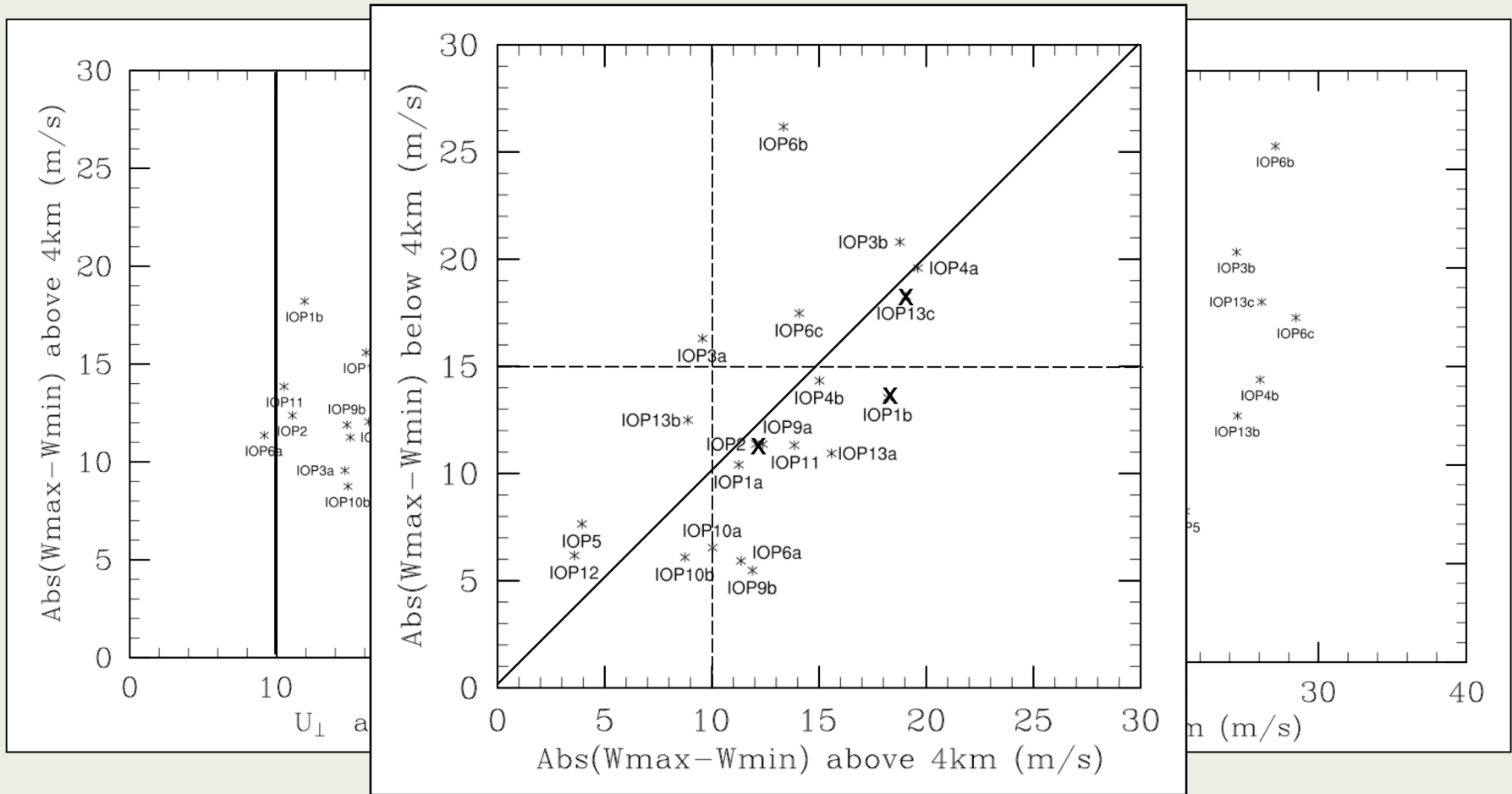


May 29, 2008

IMAGE TOY 2008 Geophysical
Turbulence Phenomena

12

All Flights 1Hz Data

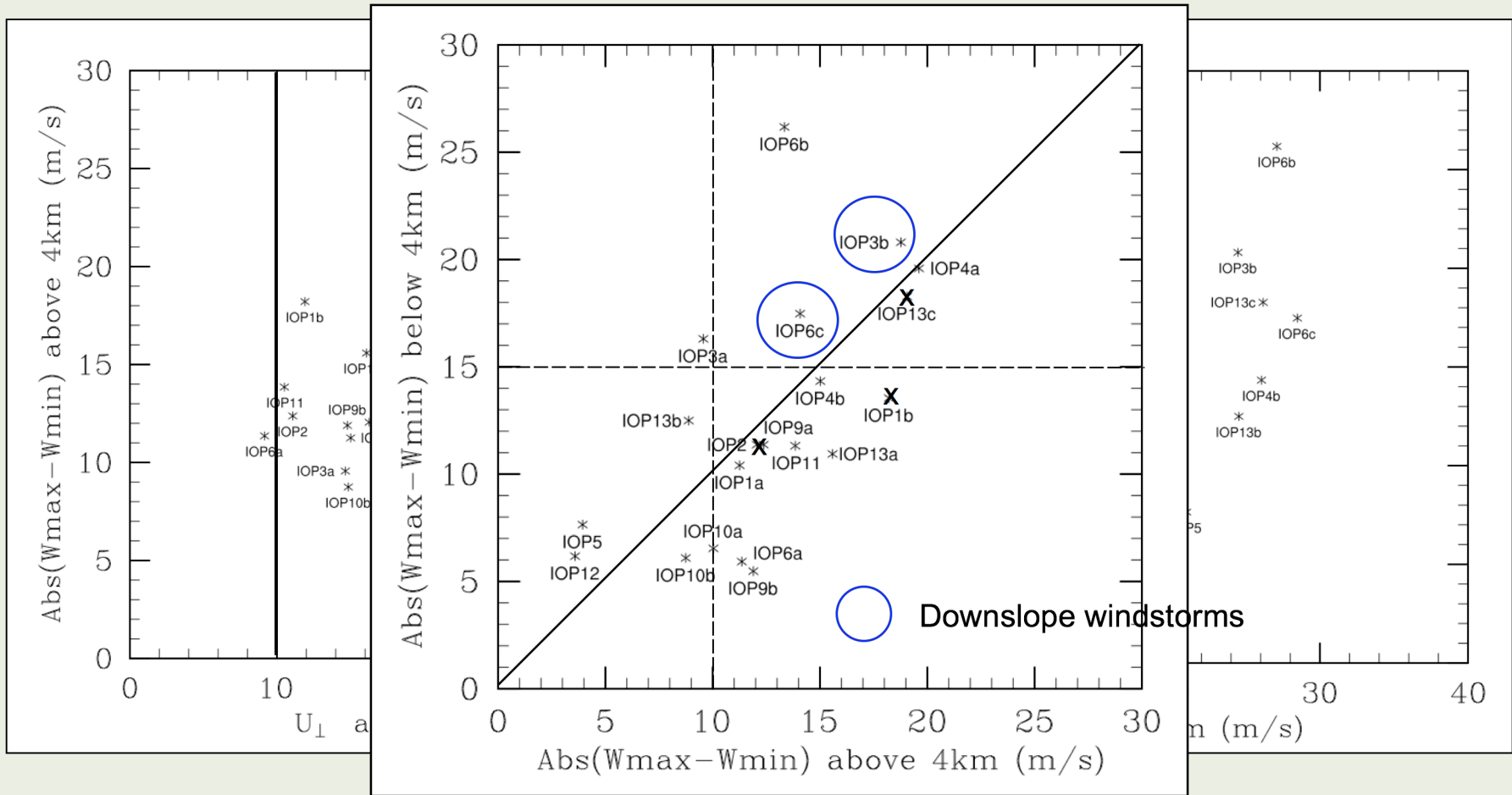


May 29, 2008

IMAGE TOY 2008 Geophysical
Turbulence Phenomena

12

All Flights 1Hz Data

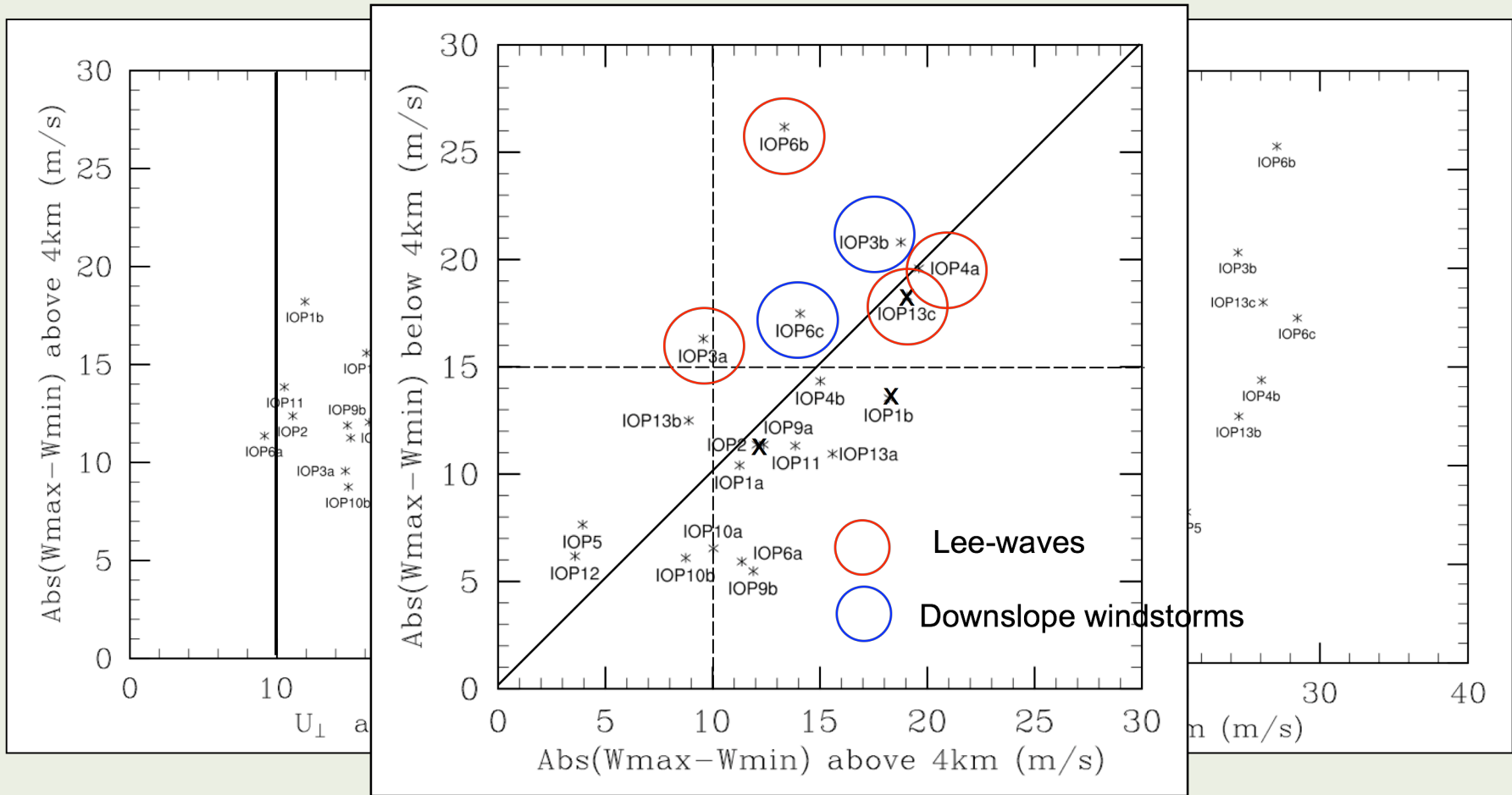


May 29, 2008

IMAGE TOY 2008 Geophysical
Turbulence Phenomena

12

All Flights 1Hz Data



Turbulence Spatial Structures

Streamlines

Turbulence Dissipation Rate from 25 Hz data

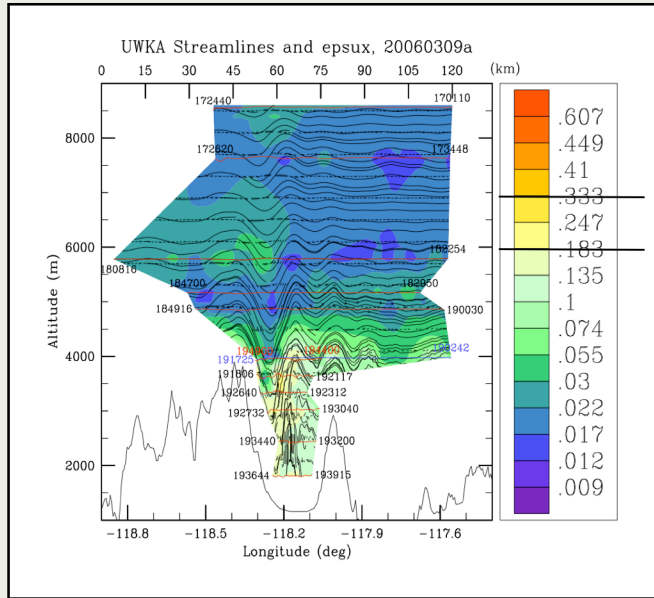
$\epsilon^{1/3} [\text{m}^{2/3}\text{s}^{-1}]$

Lester and Fingerhut (1974)

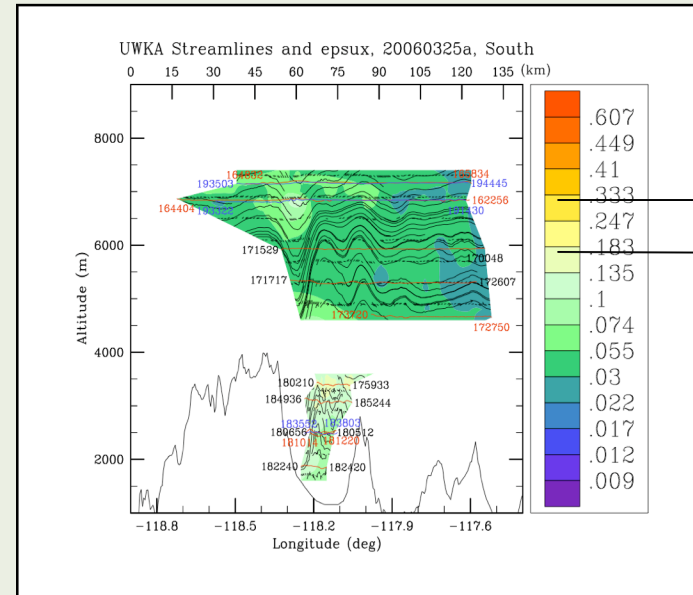
Light	0.088 – 0.188	$\text{m}^{2/3}\text{s}^{-1}$
Moderate	0.229 – 0.314	$\text{m}^{2/3}\text{s}^{-1}$
Severe	0.351 – 0.459	$\text{m}^{2/3}\text{s}^{-1}$

Lee-Waves

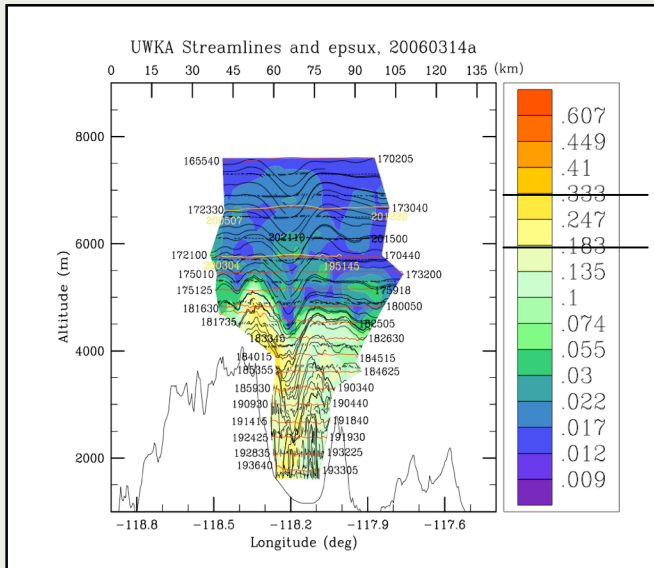
IOP 3a



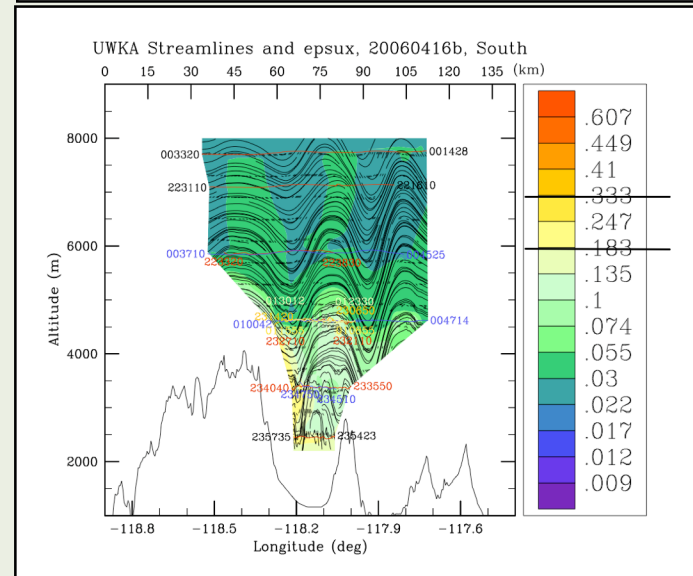
IOP 6



IOP 4a



IOP 13



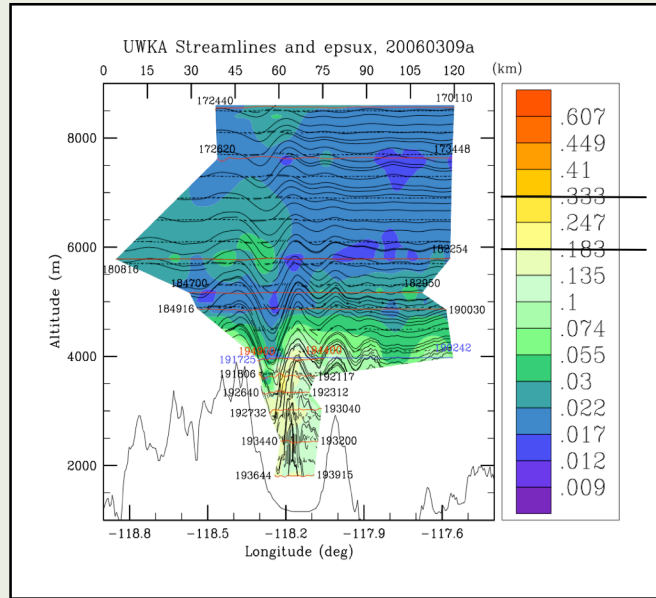
May 29, 2008

IMAGe TOY 2008 Geophysical
Turbulence Phenomena

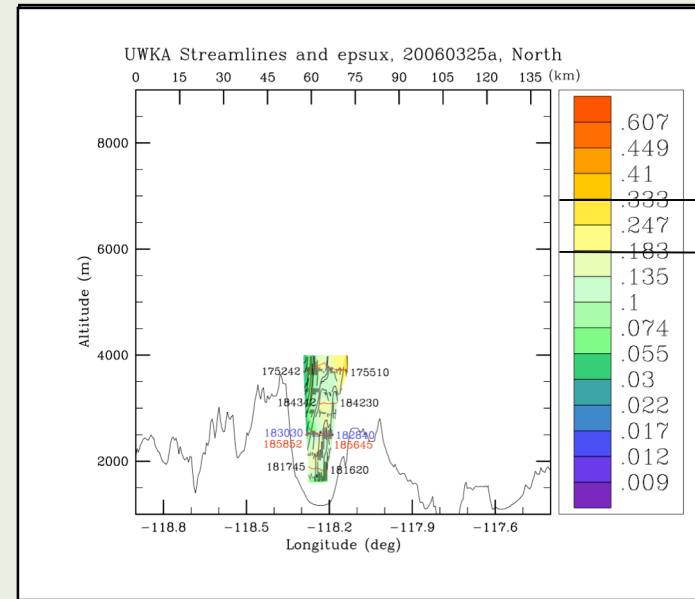
14

Lee-Waves

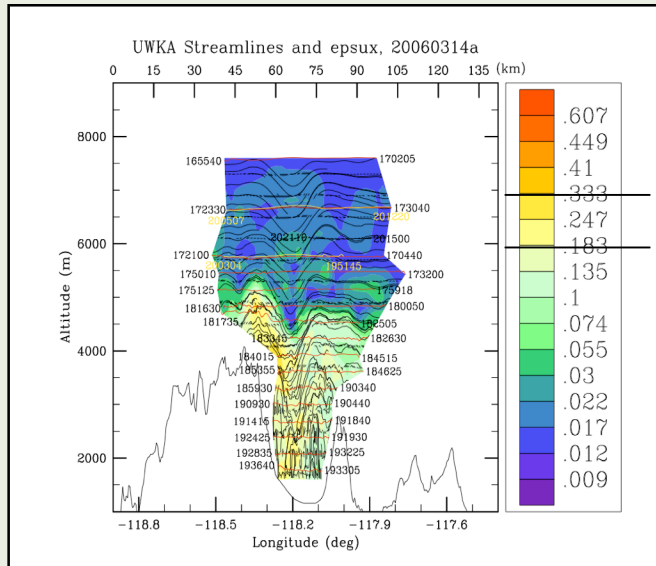
IOP 3a



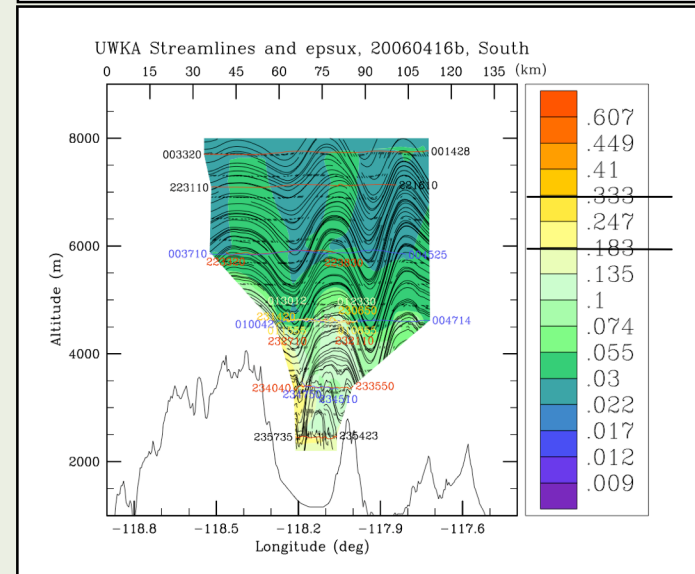
IOP 6



IOP 4a



IOP 13



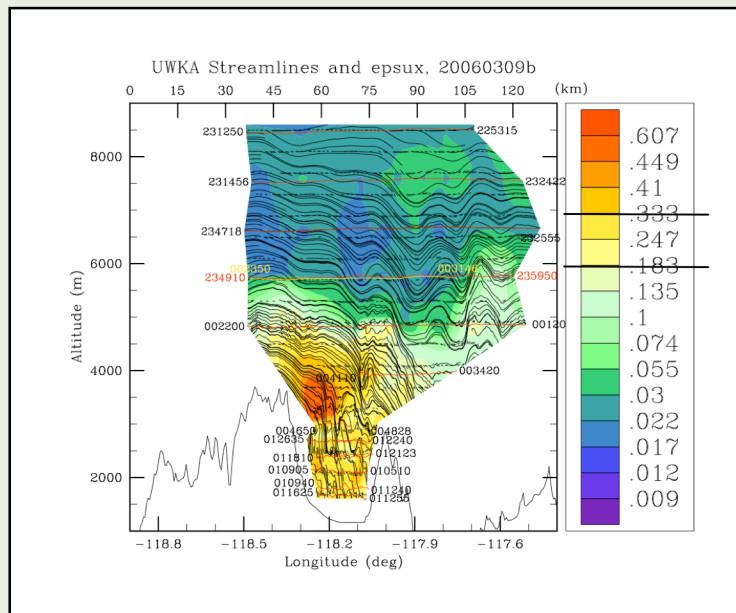
May 29, 2008

IMAGe TOY 2008 Geophysical
Turbulence Phenomena

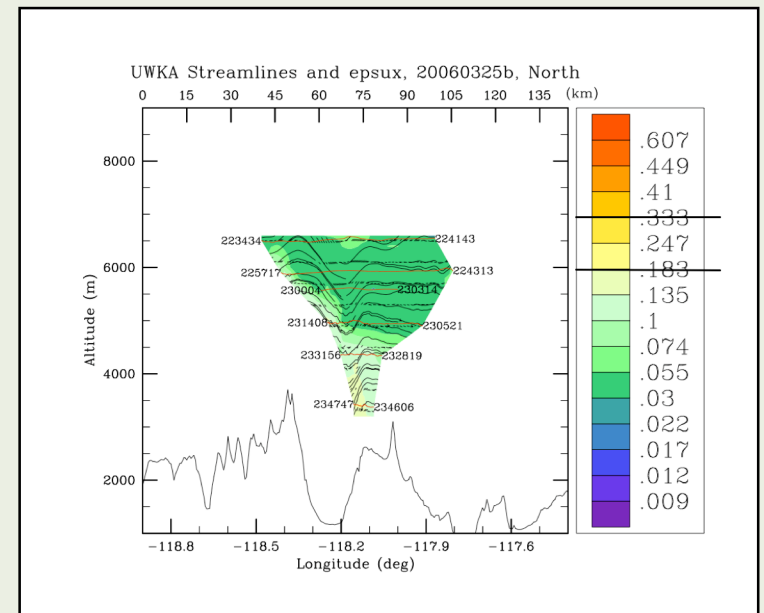
14

“Downslope Windstorms”

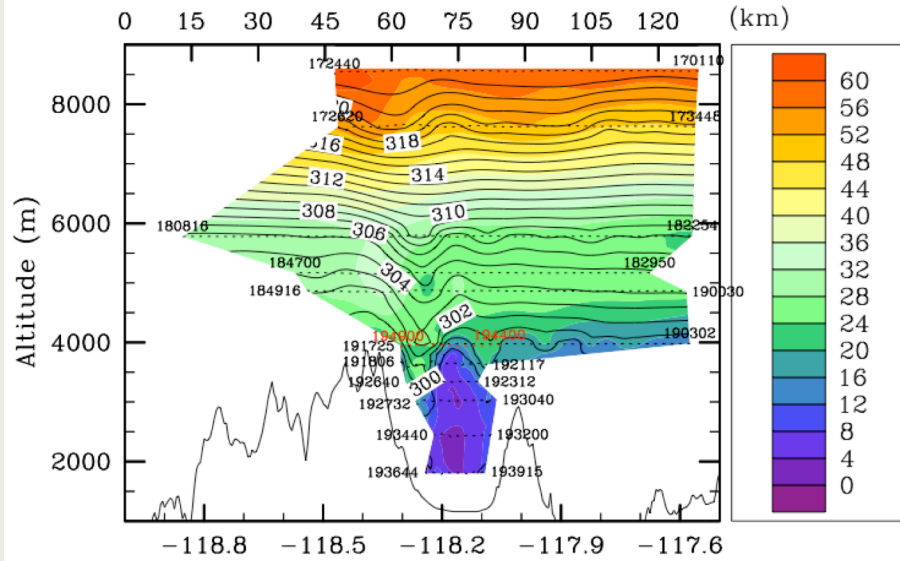
IOP 3b



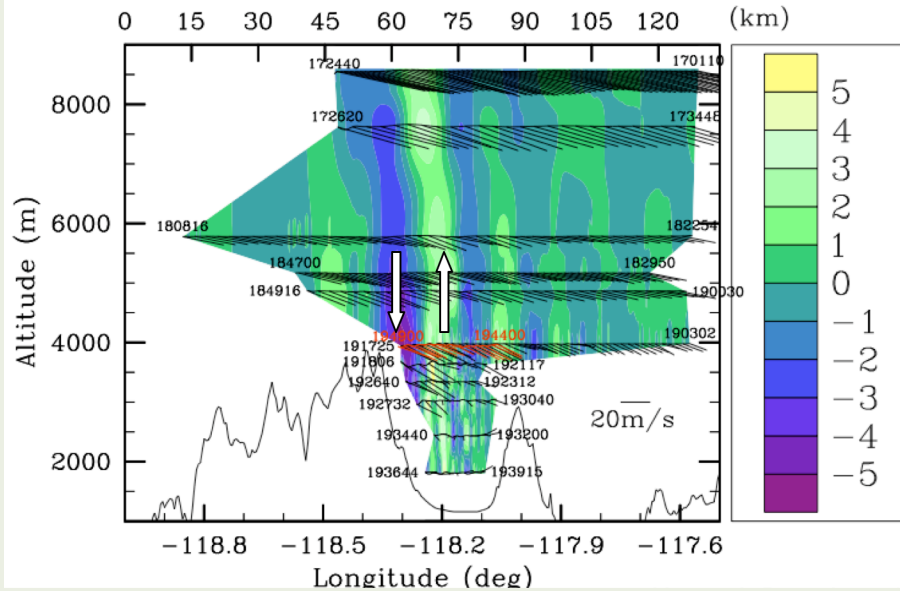
IOP 6c



UWKA WS(ms⁻¹) and Θ(K), 20060309a

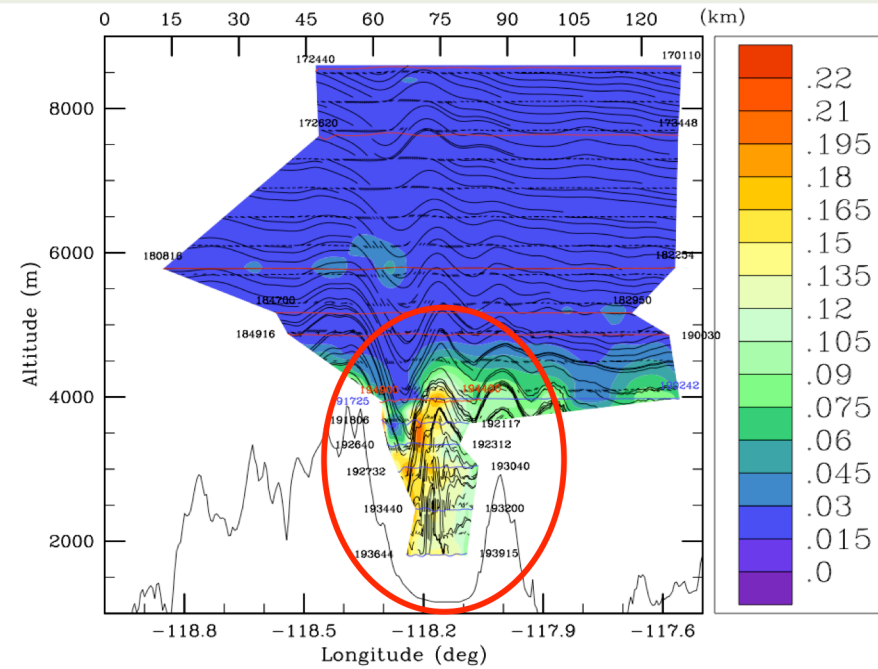


UWKA w(ms⁻¹) and wind vectors, 20060309a



IOP 3a

$$\epsilon^{1/3} [m^{2/3}s^{-1}]$$

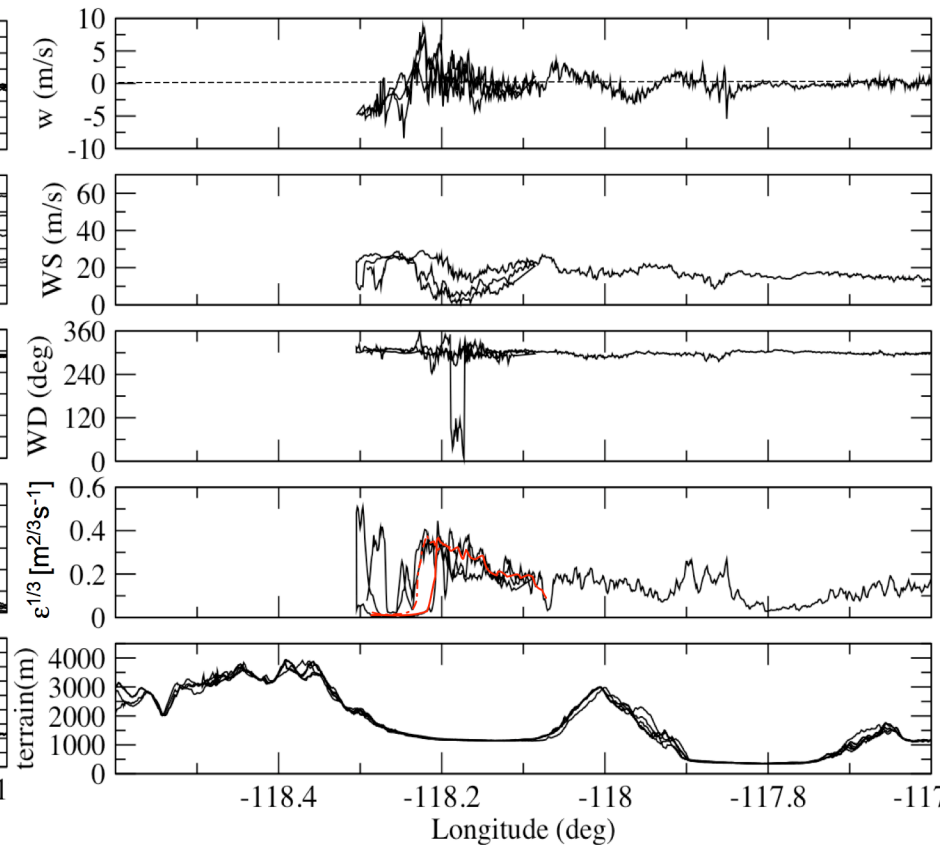
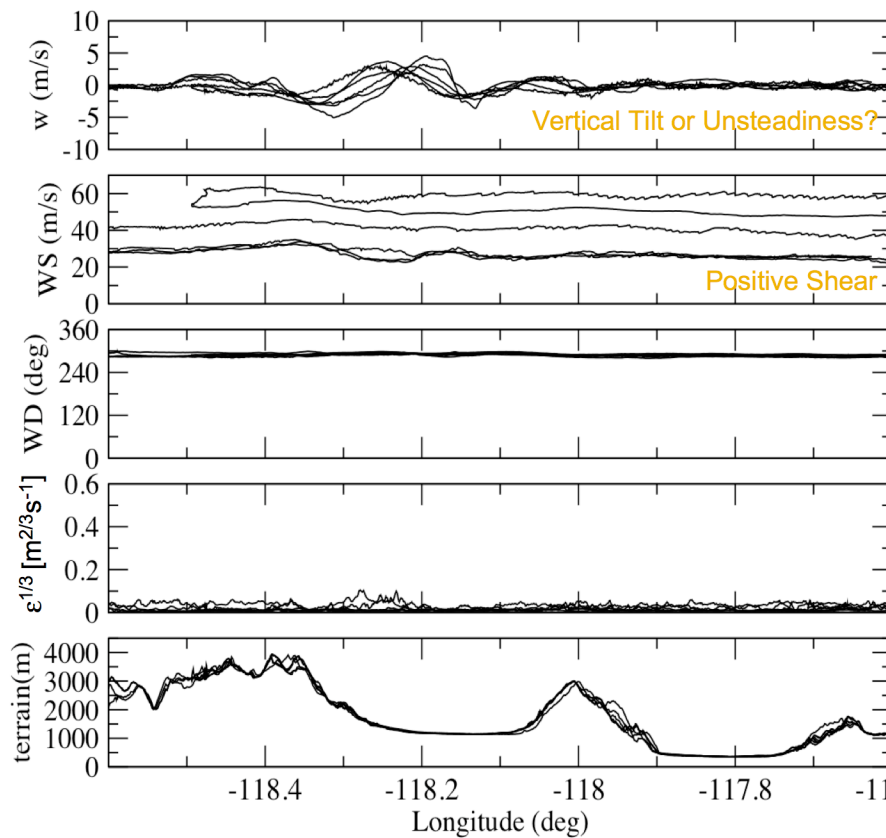


Mesoscale Dynamics and Modeling Laboratory
Vanda.Grubicic@dri.edu

IOP 3a Aircraft Data

16:57 - 19:00 UTC
4.8 - 8.6 km ASL Track A
Waves

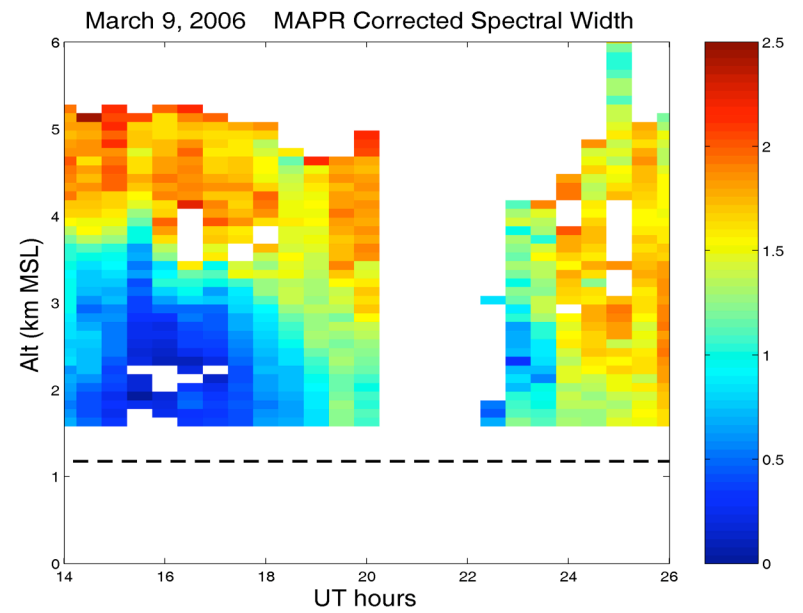
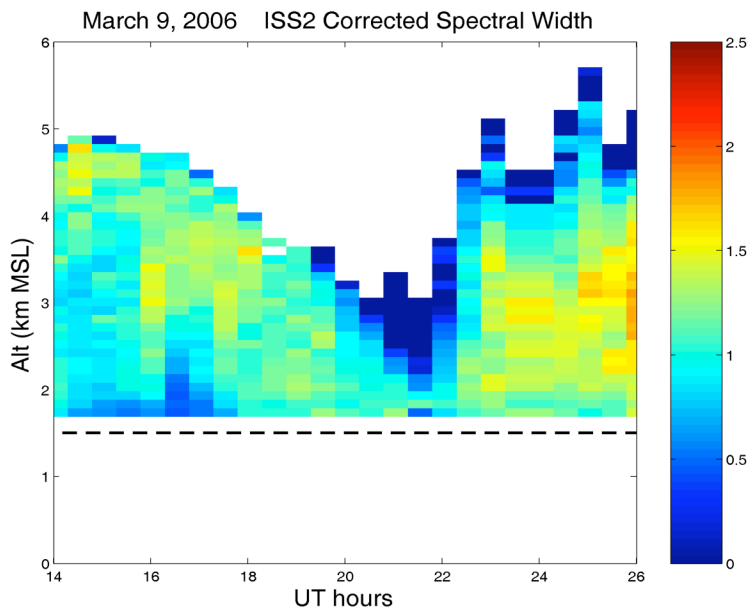
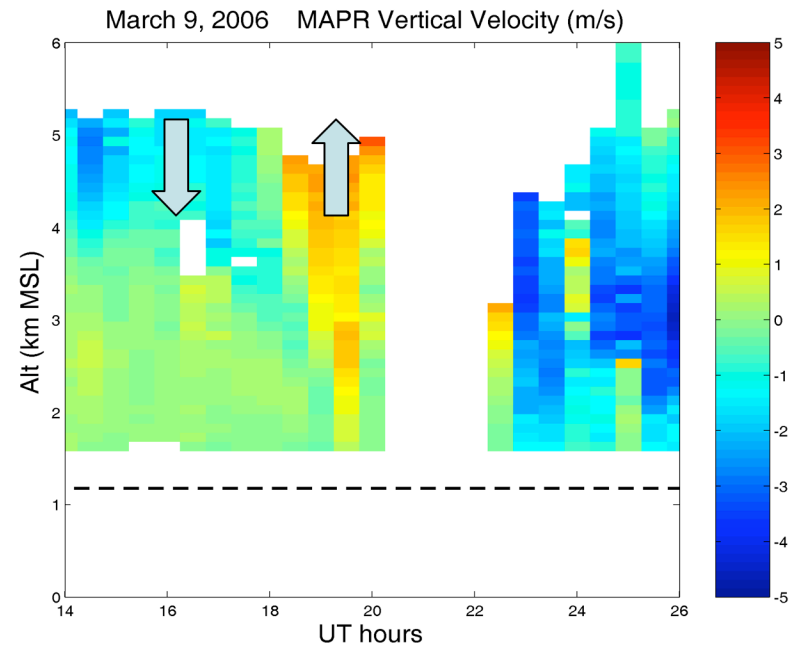
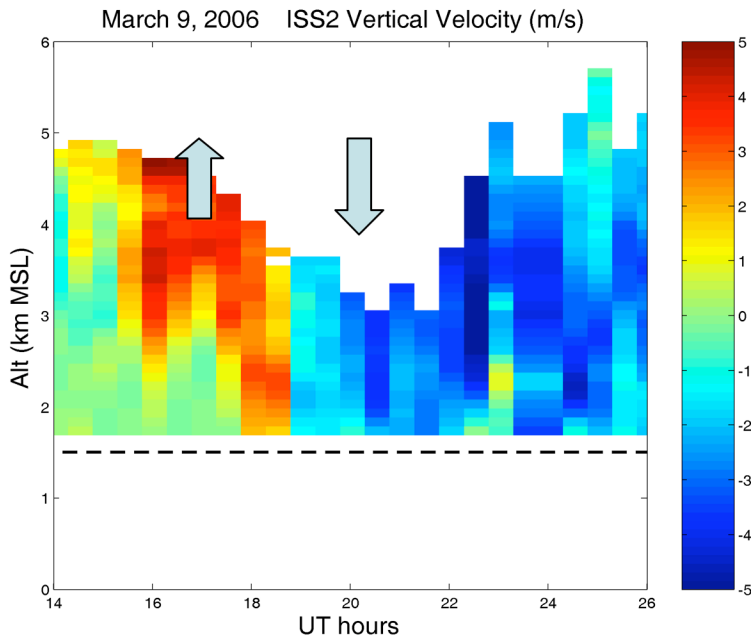
19:03 - 19:26 UTC
3.5 - 4.0 km ASL Track A
Rotor



May 29, 2008

IMAGe TOY 2008 Geophysical
Turbulence Phenomena

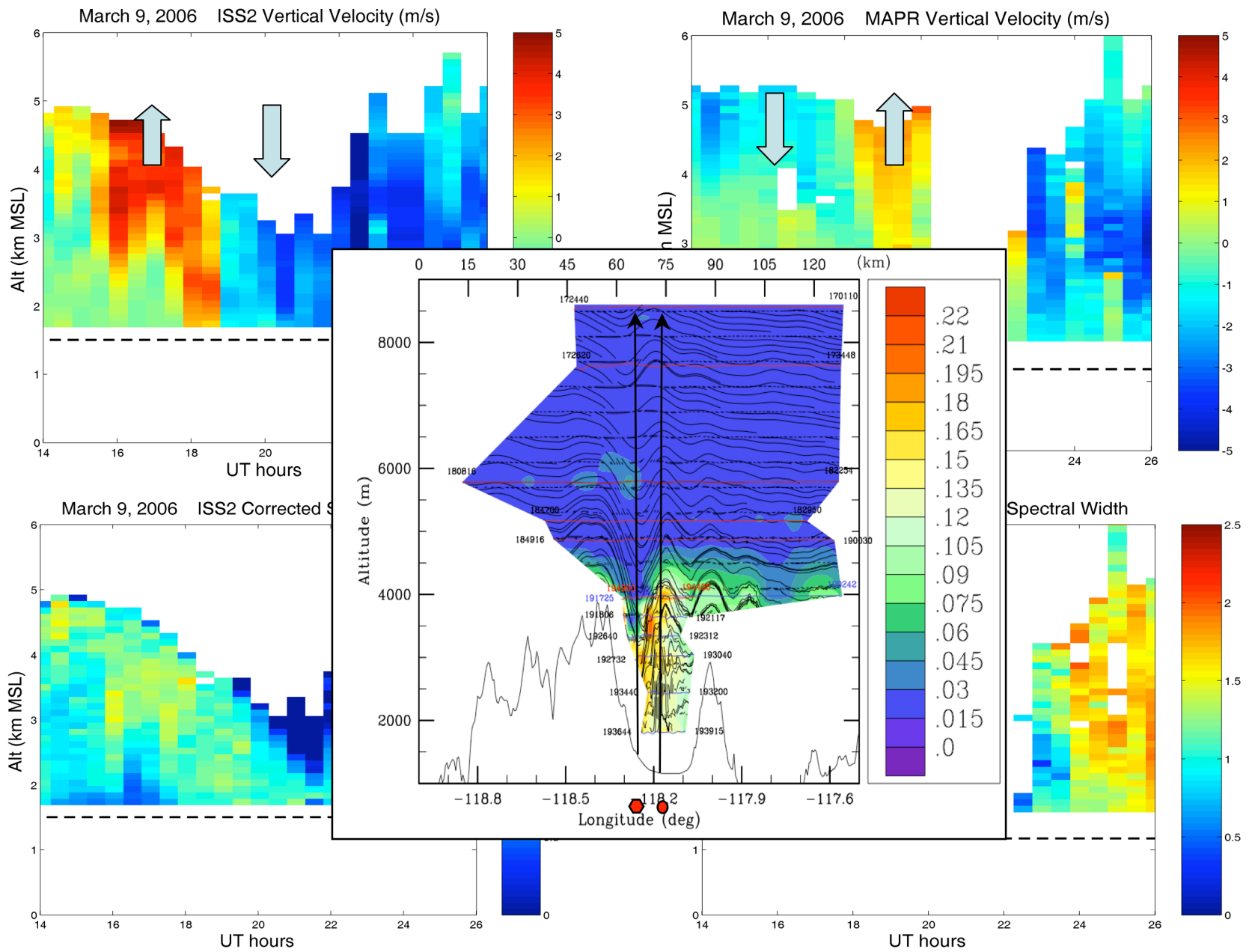
17



May 29, 2008

IMAGE TOY 2008 Geophysical
Turbulence Phenomena

18



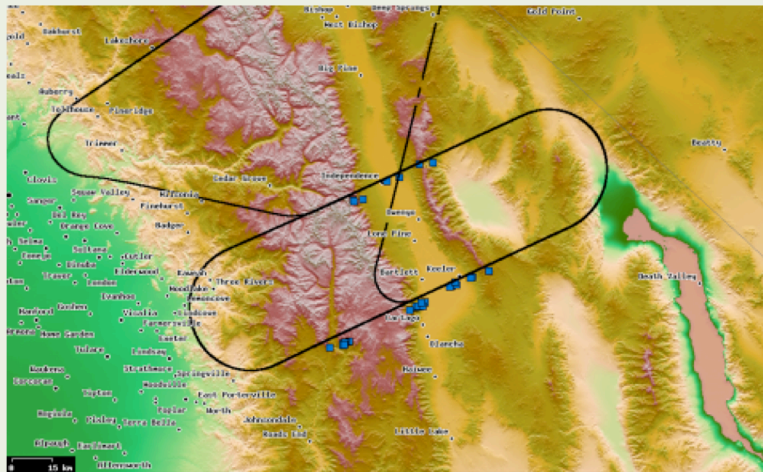
May 29, 2008

IMAGE TOY 2008 Geophysical
Turbulence Phenomena

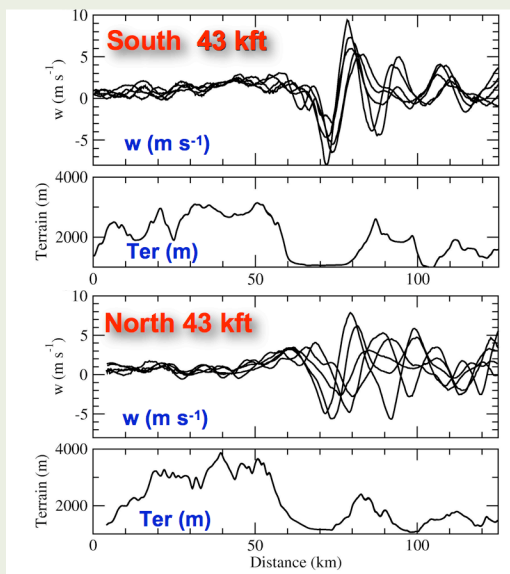
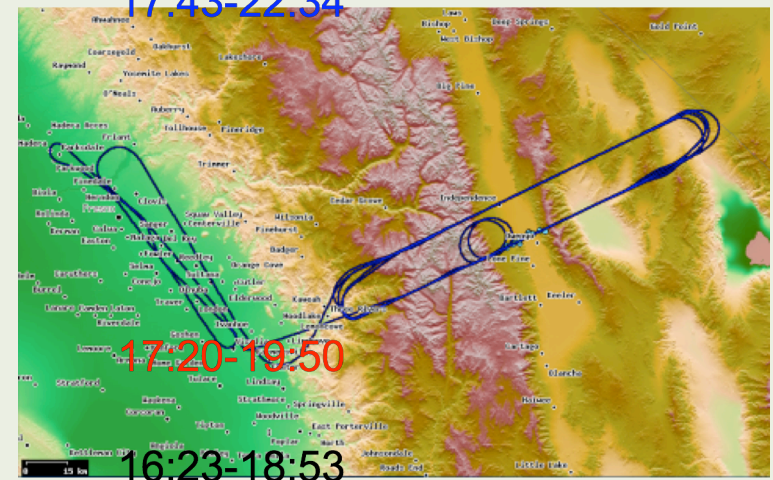
18

T-REX IOP 6 Coordinated Three-Aircraft Mission

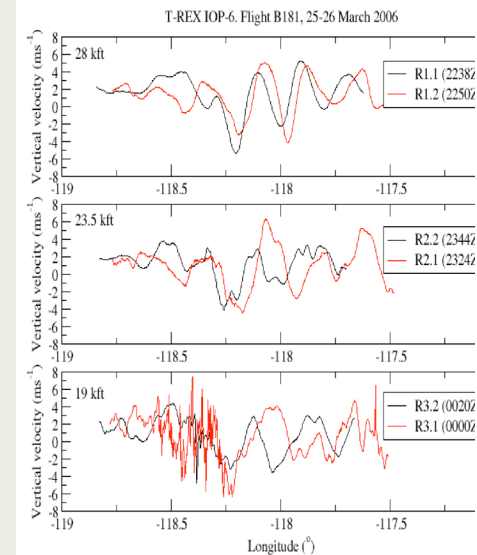
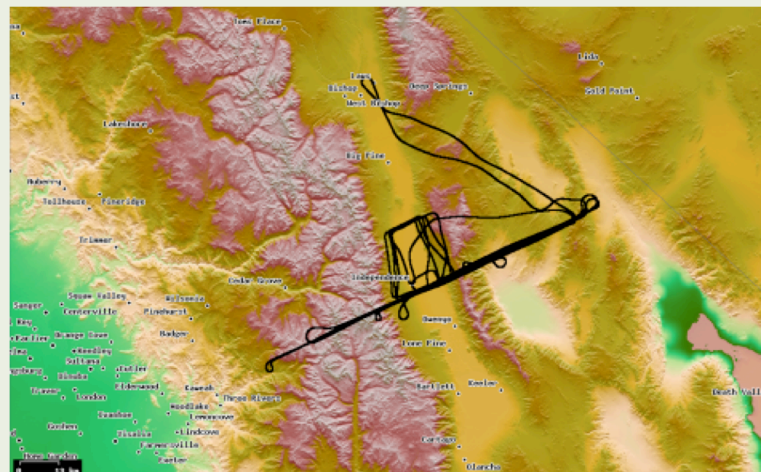
HIAPER 1 RF (RF05) Mar 25



BAe146 3 RF (B179-181) Mar 24 & 25



UWKA 3 RF Mar 24 & 25

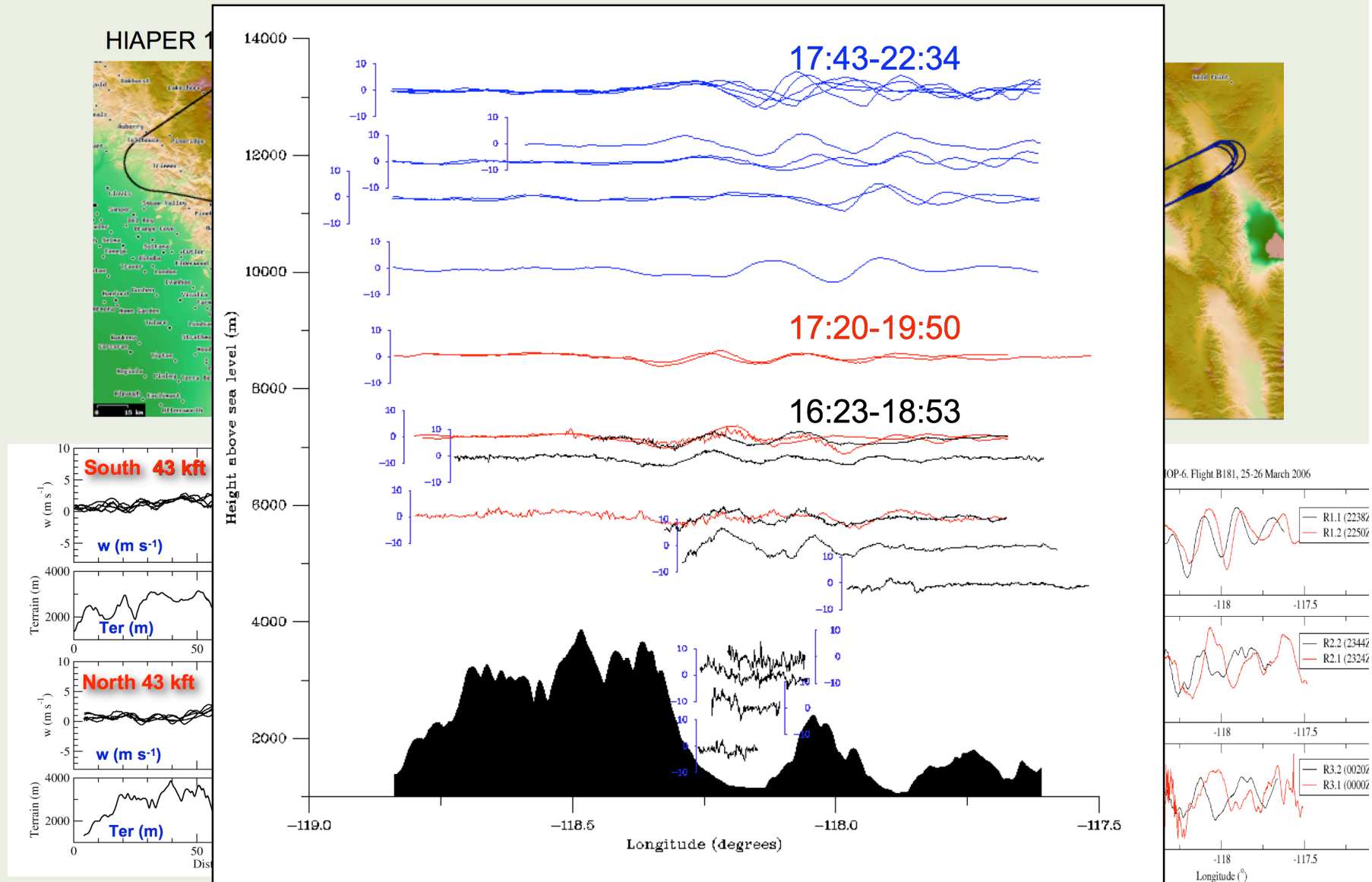


May 29, 2008

IMAGE TOY 2008 Geophysical
Turbulence Phenomena

19

T-REX IOP 6 Coordinated Three-Aircraft Mission



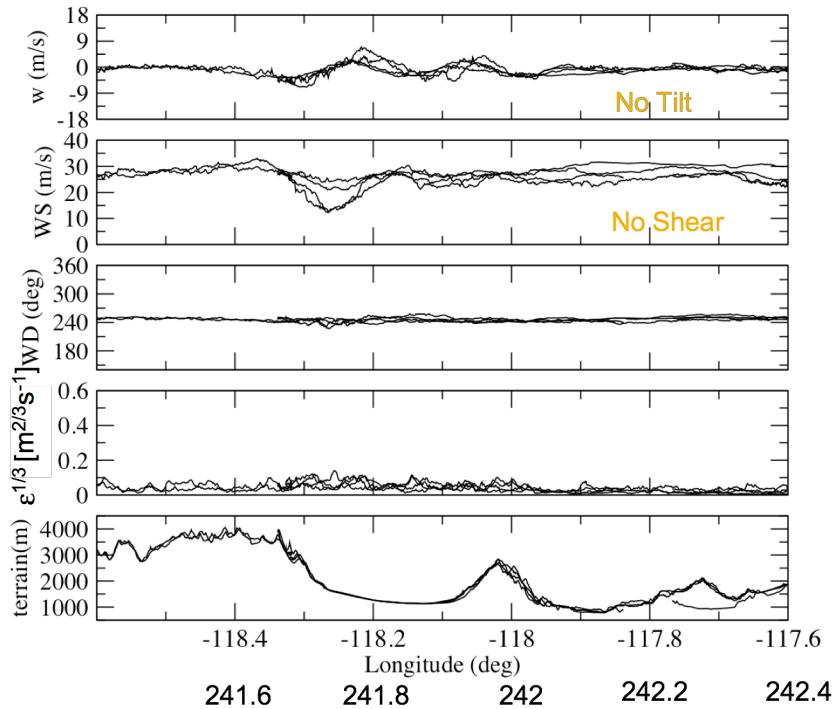
May 29, 2008

IMAGe TOY 2008 Geophysical
Turbulence Phenomena

IOP 6 Aircraft Data

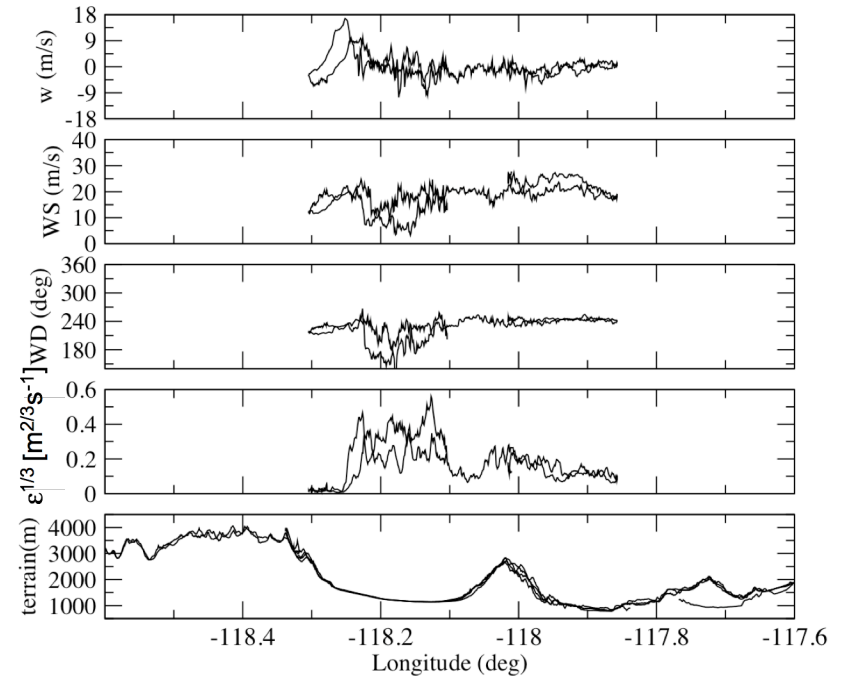
16:23 - 17:26 UTC

5.3 - 7.2 km ASL Track B
Above Rotor and Cap Clouds



17:41 - 17:59 UTC

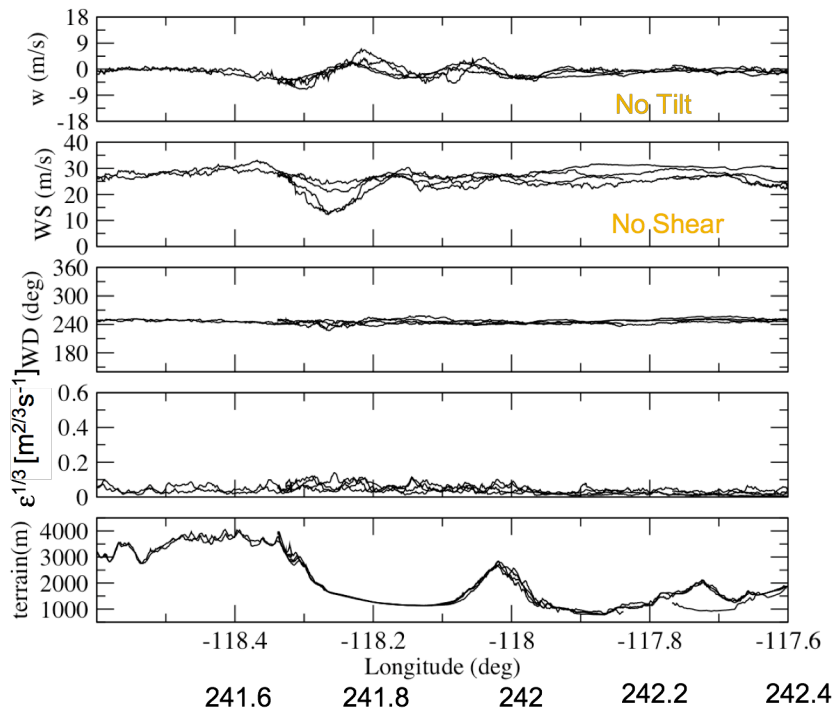
3.9 km ASL Track B & Box
Below Rotor Cloud Base



IOP 6 Aircraft Data

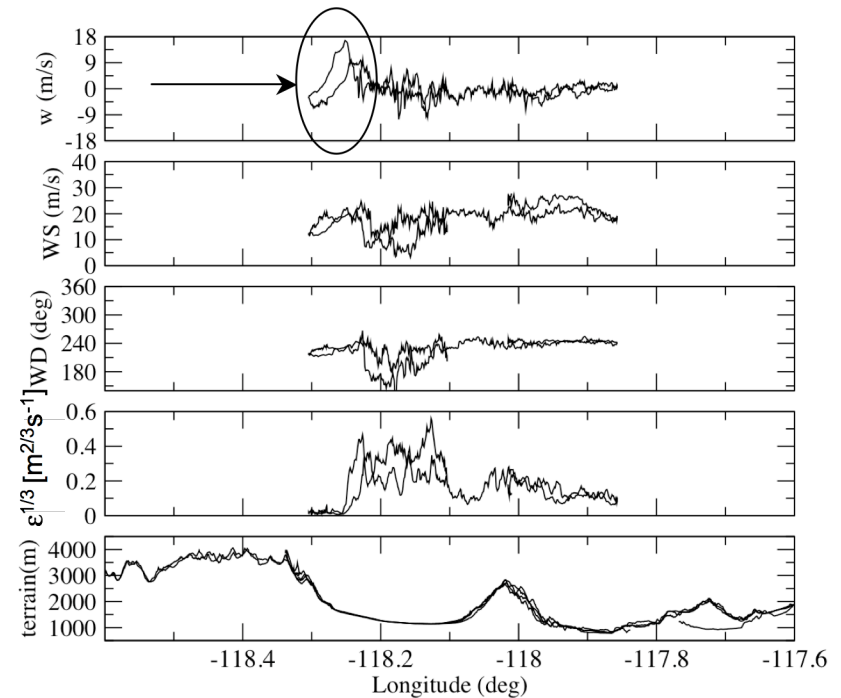
16:23 - 17:26 UTC

5.3 - 7.2 km ASL Track B
Above Rotor and Cap Clouds



17:41 - 17:59 UTC

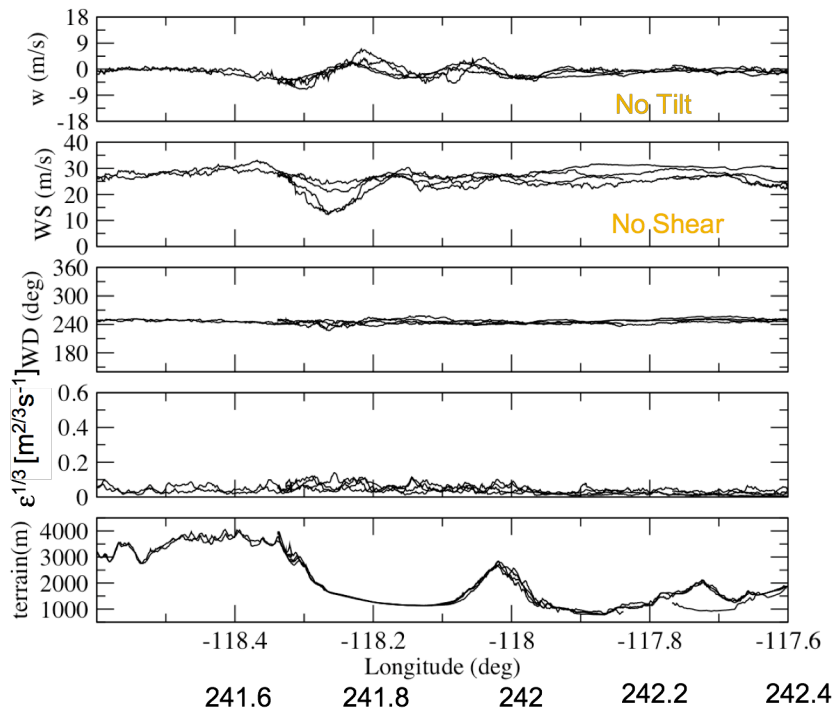
3.9 km ASL Track B & Box
Below Rotor Cloud Base



IOP 6 Aircraft Data

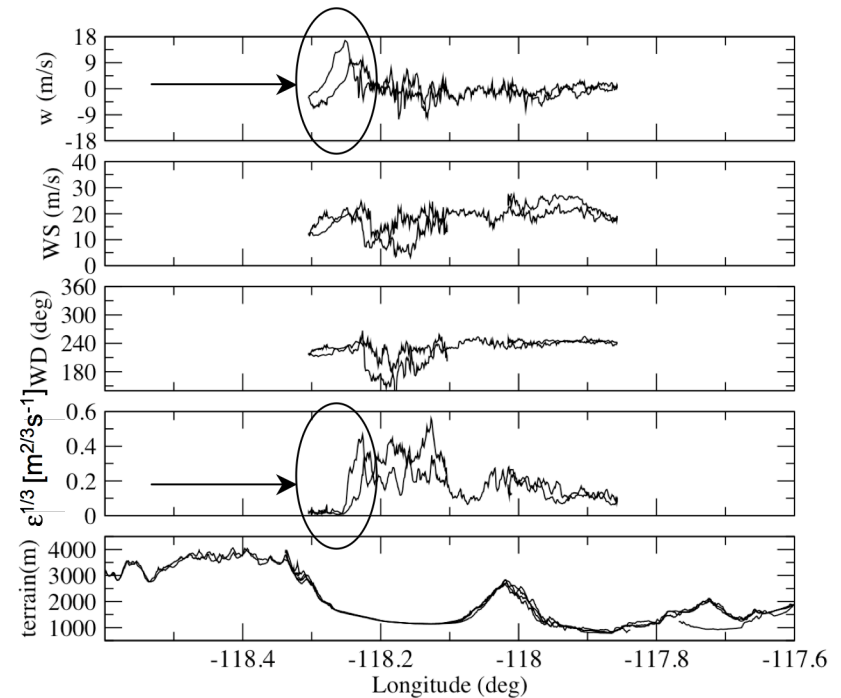
16:23 - 17:26 UTC

5.3 - 7.2 km ASL Track B
Above Rotor and Cap Clouds



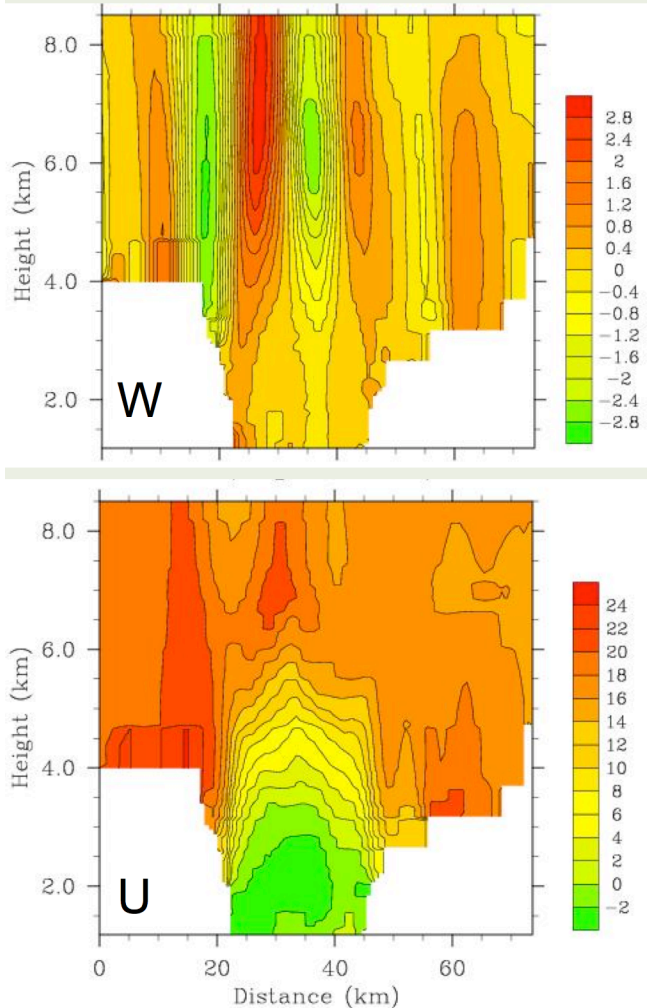
17:41 - 17:59 UTC

3.9 km ASL Track B & Box
Below Rotor Cloud Base



Turbulence Characteristics Observed Over Owens Valley (IOP 1)

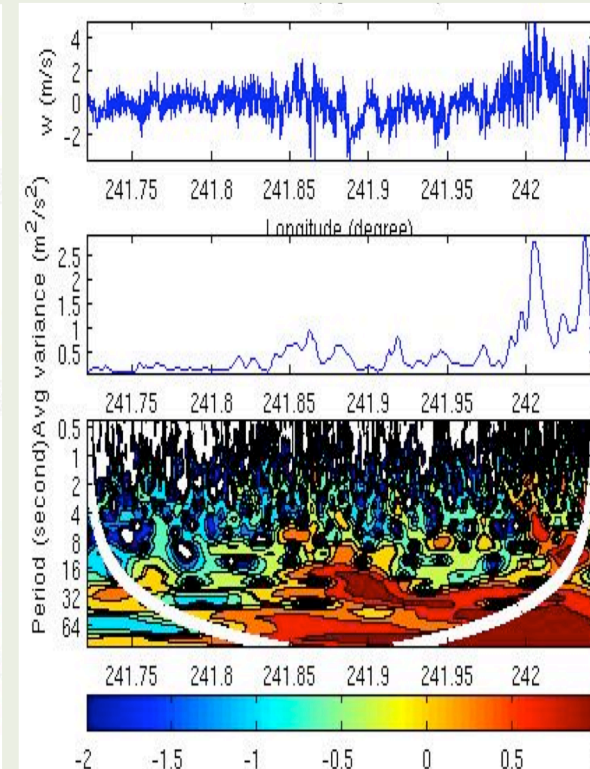
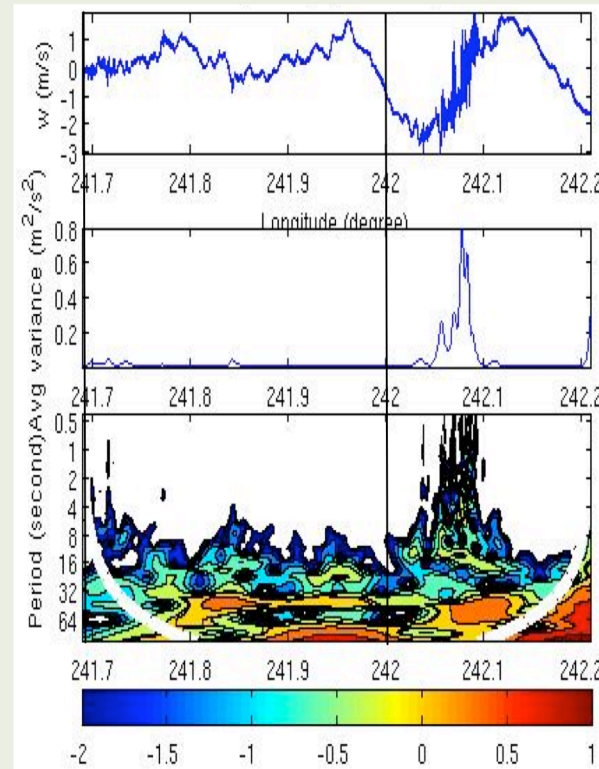
Objective Analysis of W and U of IOP 1a



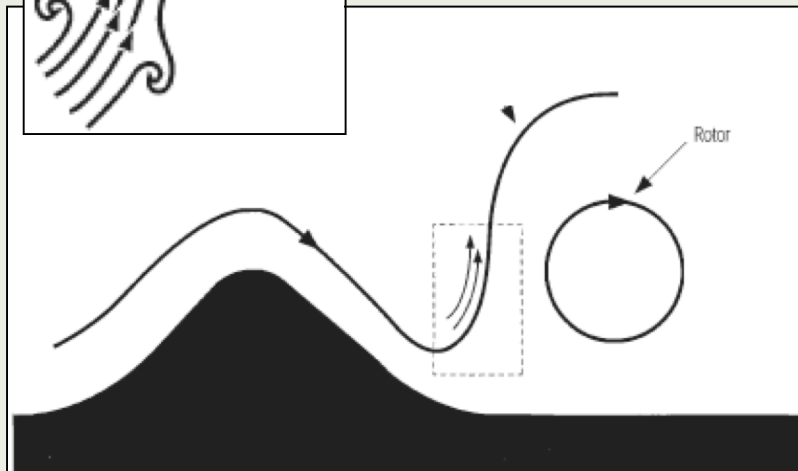
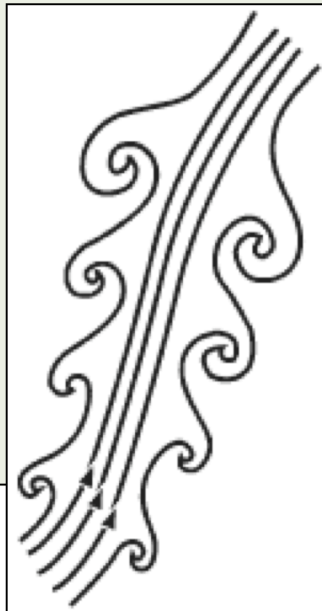
Wavelet Analysis: IOP 1a

w (m s⁻¹) at 4900 m

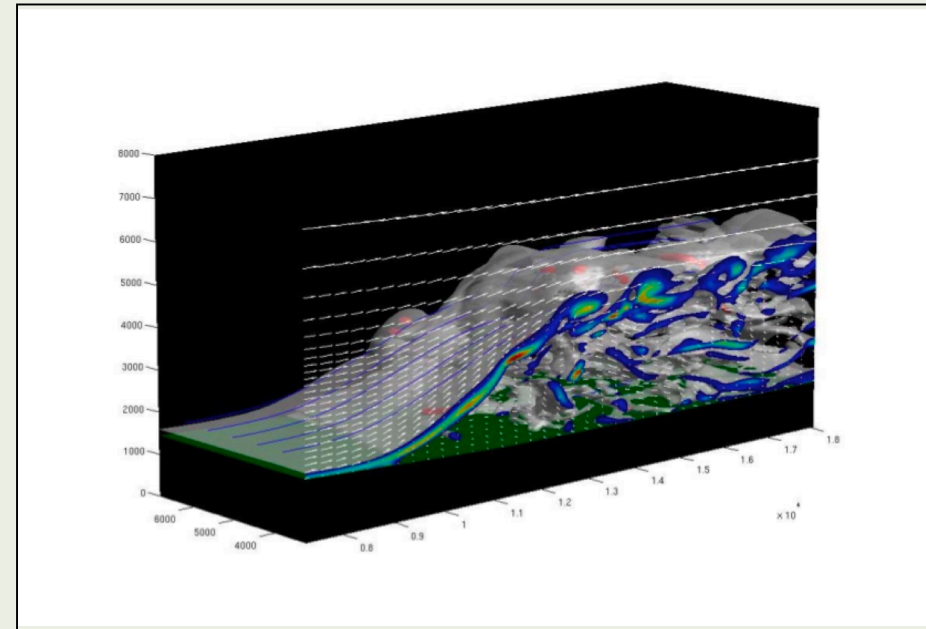
w (m s⁻¹) at 3600 m



Internal Rotor Structure: Subrotors



Doyle et al. (2008)



May 29, 2008

IMAGE TOY 2008 Geophysical
Turbulence Phenomena

22

Radiosonde: Rise rate calculation

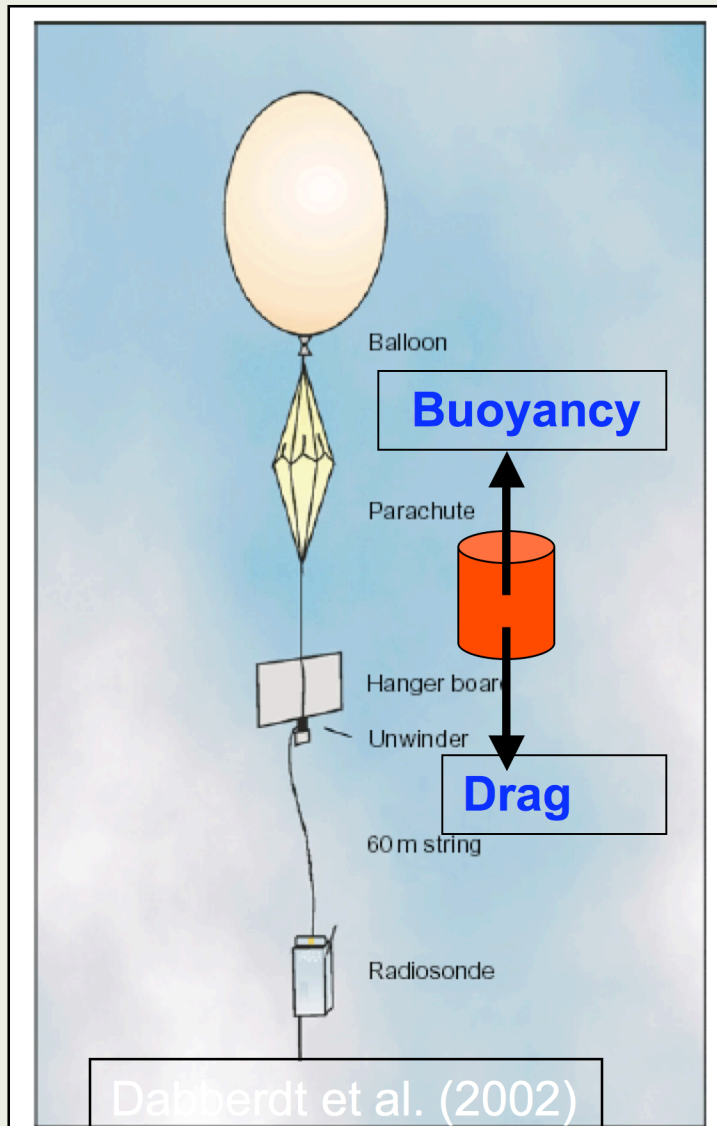


Figure 2 Typical radiosonde flight train, including balloon, parachute and hanger board, unwinder mechanism, separation line, and radiosonde.

Buoyancy force = Drag force

$$[BV\rho_s - (m_s + m_b + m_h)]*g = C_D * A * \rho * V_{rr}^2 / 2$$

$$m_h = BV * \rho * 4.0026 / 28.9644$$

$$V_{rr} = (2 * BF / C_D * A * \rho)^{1/2}$$

BV0: ~20-40 ft³ ?

m_s = 330g m_b = 200g

C_D ~ 0.2-0.5 ?

$$A = 4 * \pi * [3 * BV / (4 * \pi)]^{2/3}$$

ρ : density (kg m⁻³)

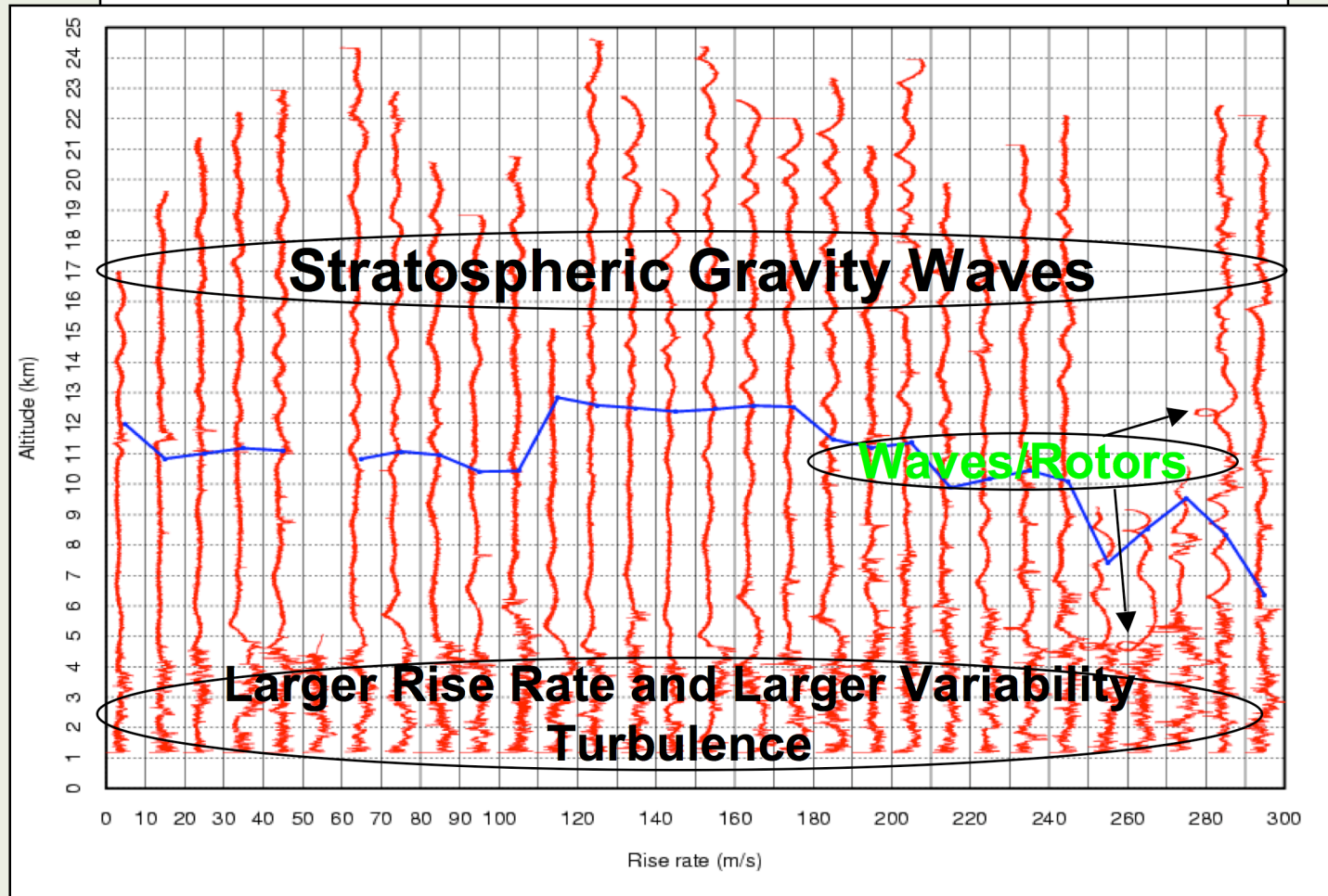
$$\text{Vertical Wind} = V_{\text{measured}} - V_{rr}$$

Factors affecting C_d (Lalas and Einaudi, 1980)

1. The radiosonde balloon is not super-pressurized, so does not retain the spherical shape. For $Re=10^5$, $C_d = \sim 0.5$ for a sphere, $C_d = 1.2$ for a semi-sphere.
2. The weight of the instrument package results in some stretching of the bottom part, which leads to a shape with a conical afterbody and then reduce C_d .
3. The balloon motion in the atmosphere lies in a flow regime with Re close to the critical value of 2.5×10^5 , near which C_d experiences drastic changes.
4. The free stream turbulence and unsteadiness affects C_d .
5. The dependence of C_d on the effective radius of the balloon, which is almost impossible to estimate.

T-REX Valley Soundings 1Hz Data

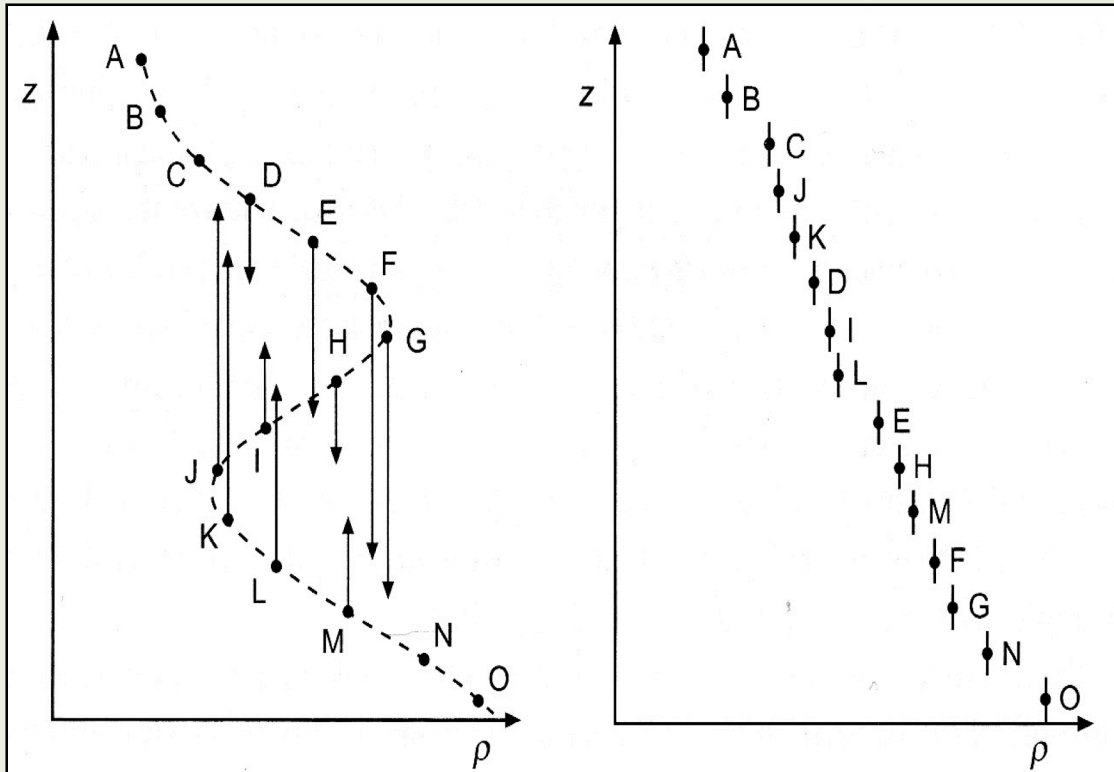
GAUS-ISS (March 2006; Soundings 1-30)



May 29, 2008

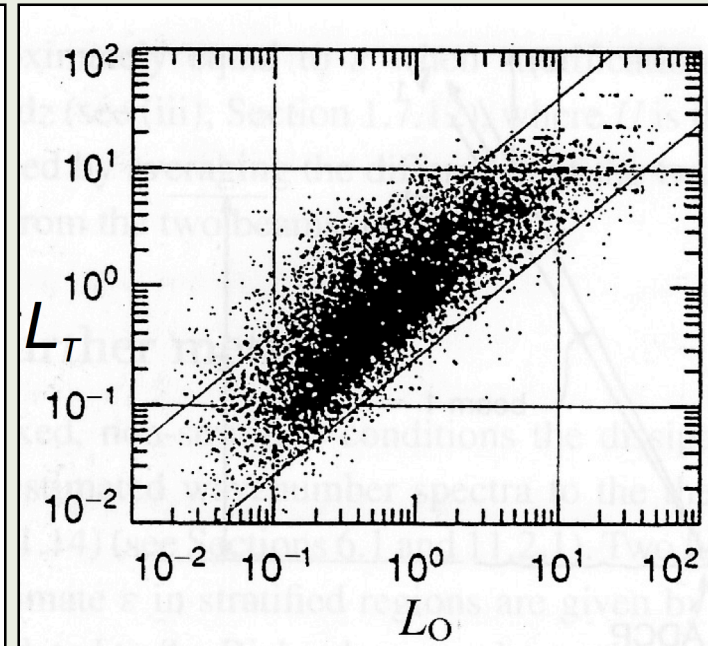
IMAGE TOY 2008 Geophysical
Turbulence Phenomena

25



(a) Thorpe (2005) (b)

Figure 6.2. The sorting algorithm. This is used to create a stable profile of density with $d\rho/dz \leq 0$ shown in (b) from the observed profile, (a), in which there is a statically unstable region where $d\rho/dz > 0$. The points, A–O, represent the discrete measured values of density at their respective levels, z . Those between C and N are statically unstable in the sense that, because of the density inversion, there is denser fluid above or less dense below them even though the density only decreases with depth between G and J. The vertical lines and arrows show the displacements in z required to re-sort the observed density profile into the statically stable order shown



Ozmidov Scale (indicative of maximum overturning scale in a stably stratified fluid):

$$L_O = \varepsilon^{1/2} N^{-3/2}$$

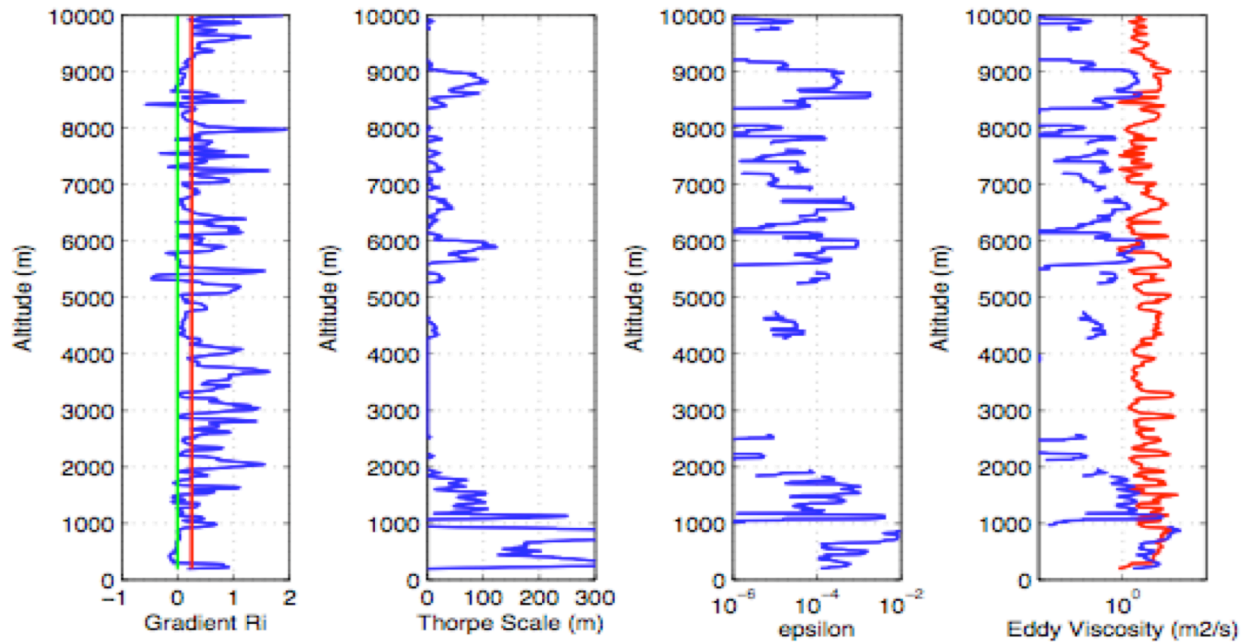
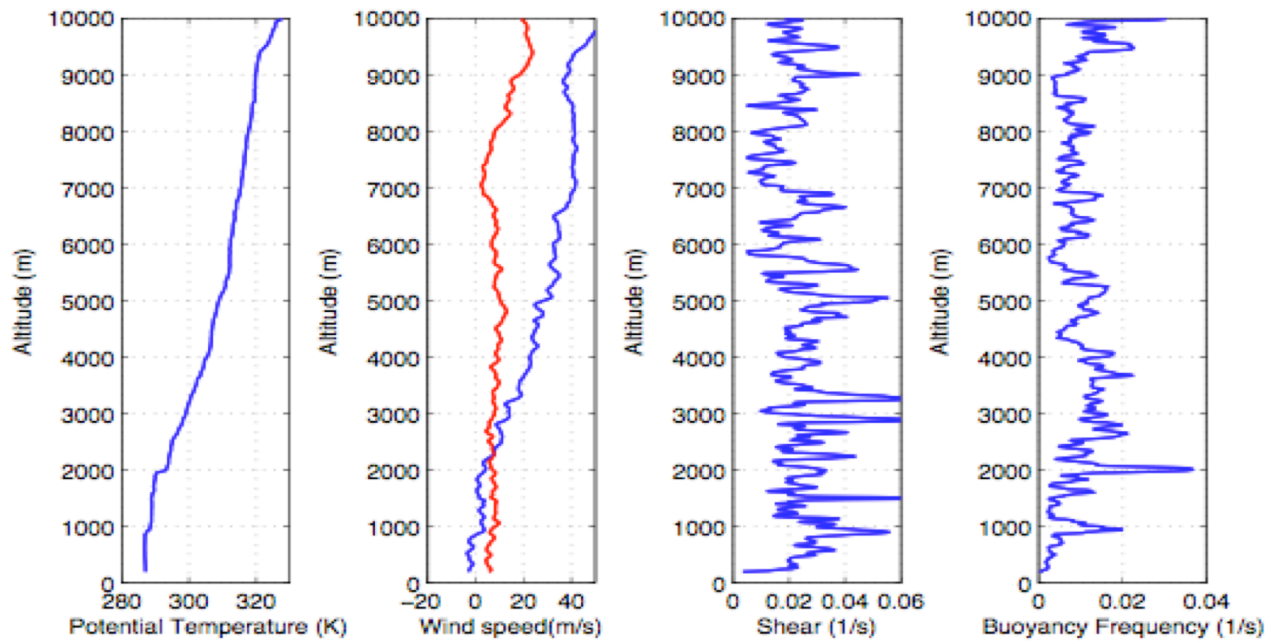
Thorpe scale $L_T \sim L_O$

Therefore TKE dissipation rate

$$\varepsilon = c_K L_T^2 N^3$$

Also Eddy Diffusivity

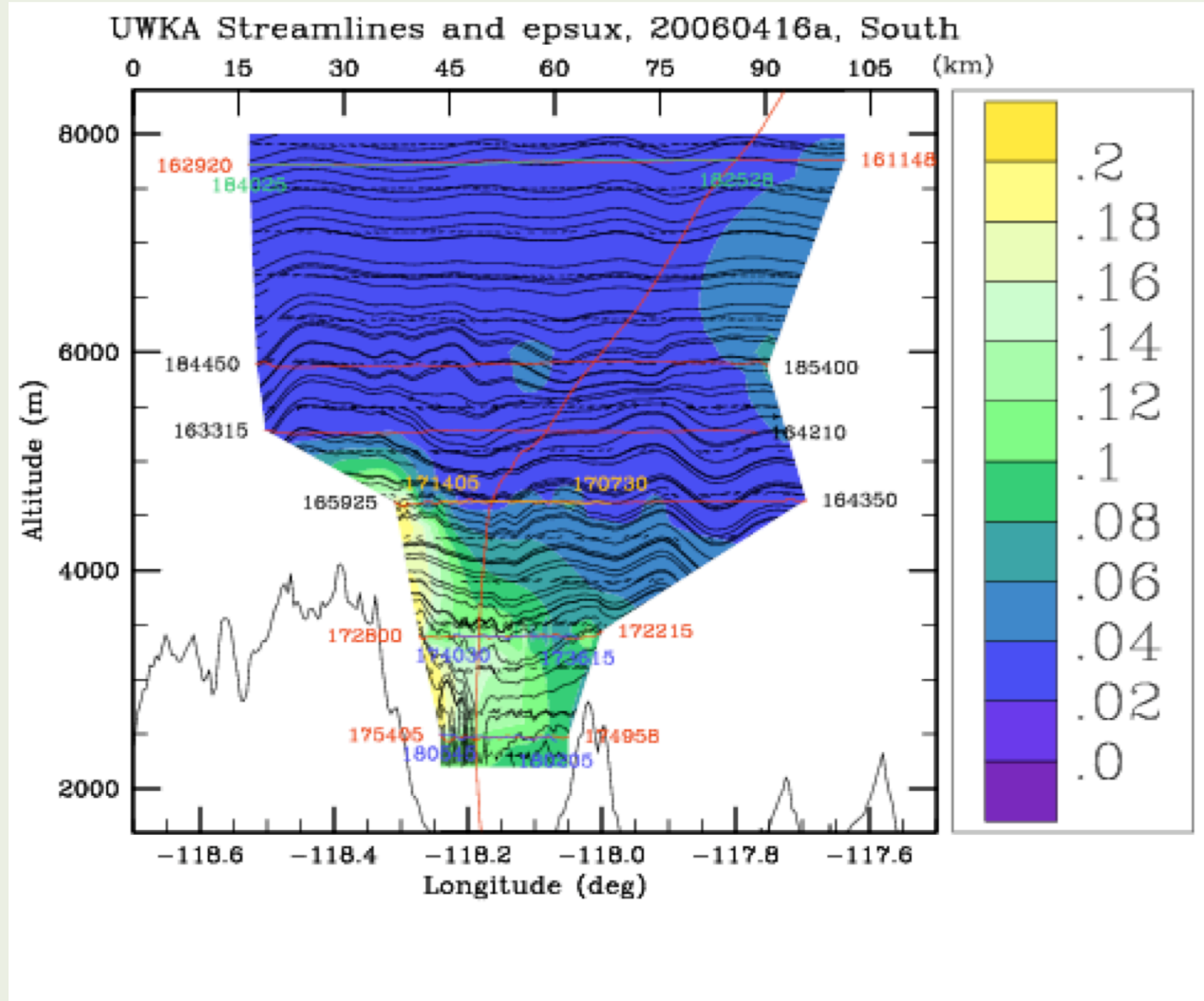
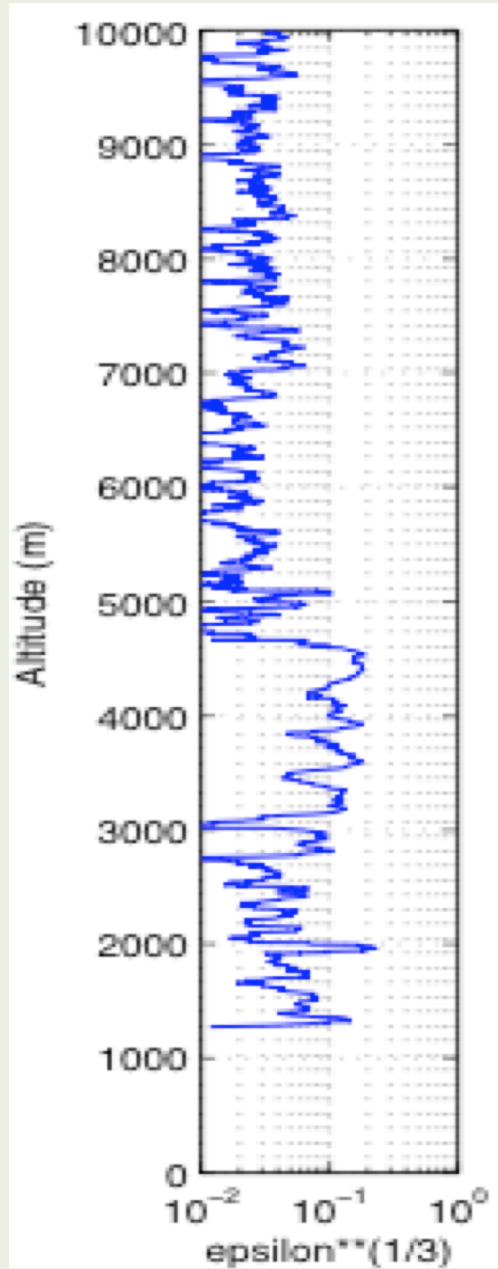
$$K = \gamma \varepsilon N^{-2}$$



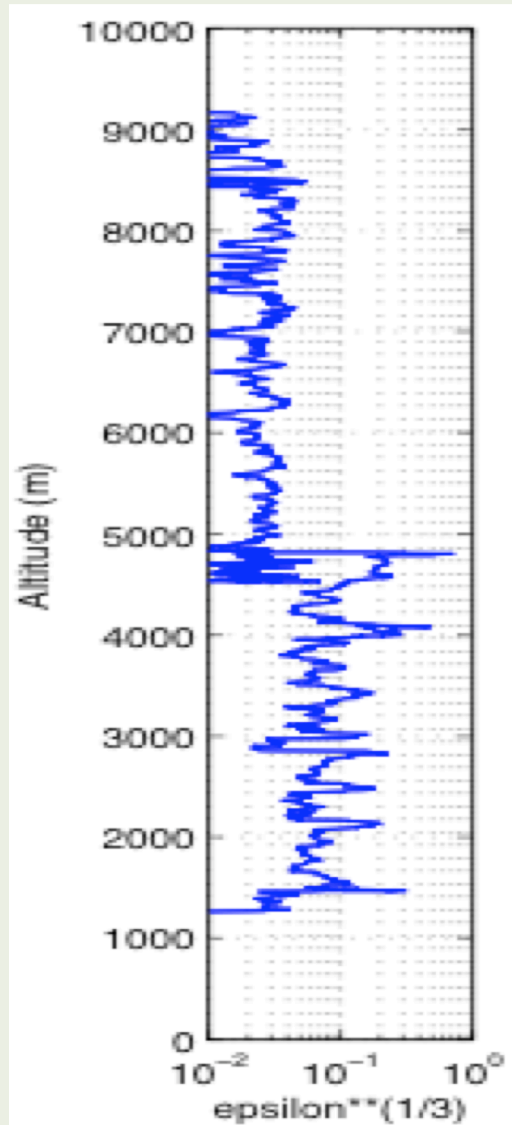
IOP 13
(April 16, 2006)

Upstream Sonde

IOP 13 (April 16, 2006)



IOP 03 (March 9, 2006)



May 29, 2008

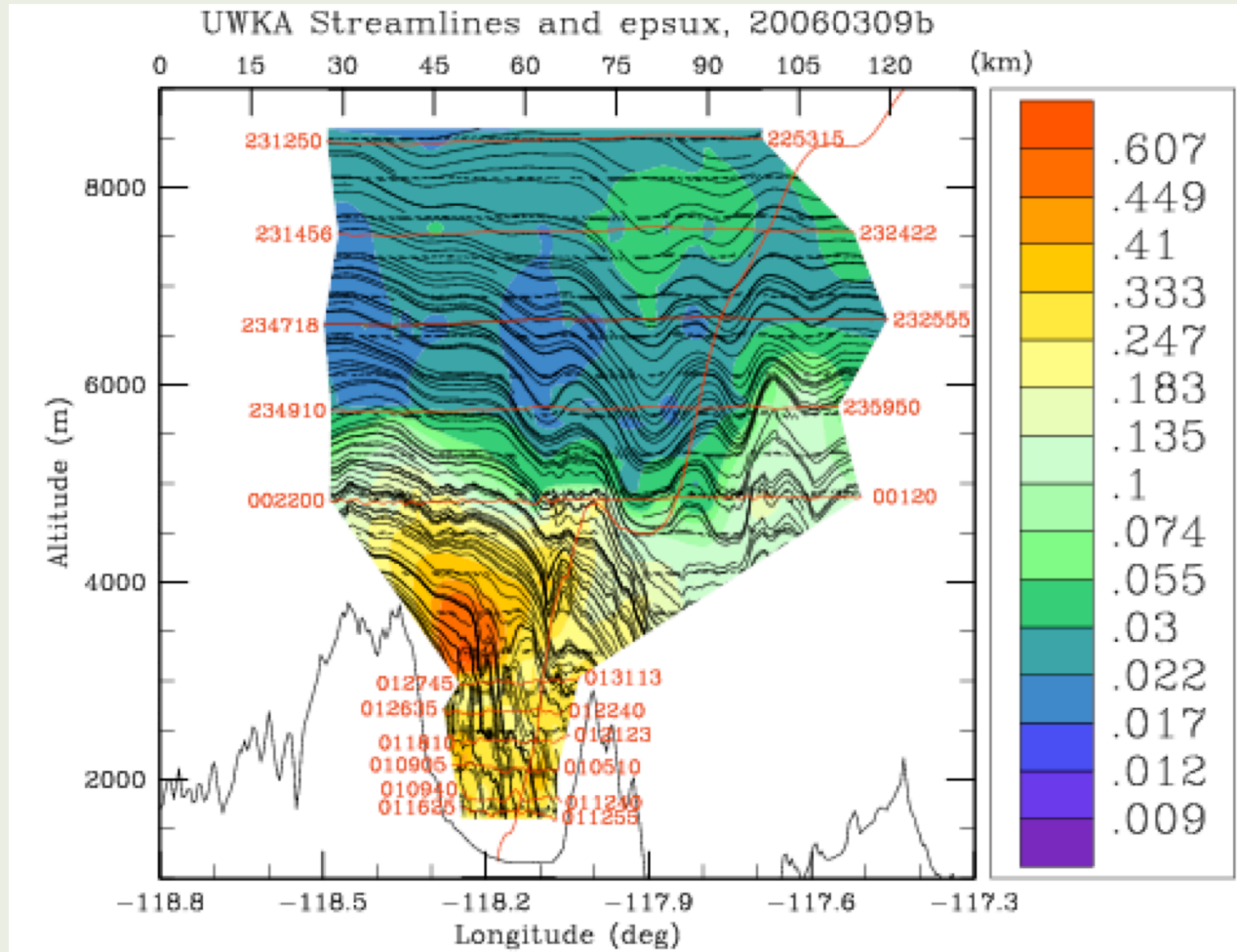
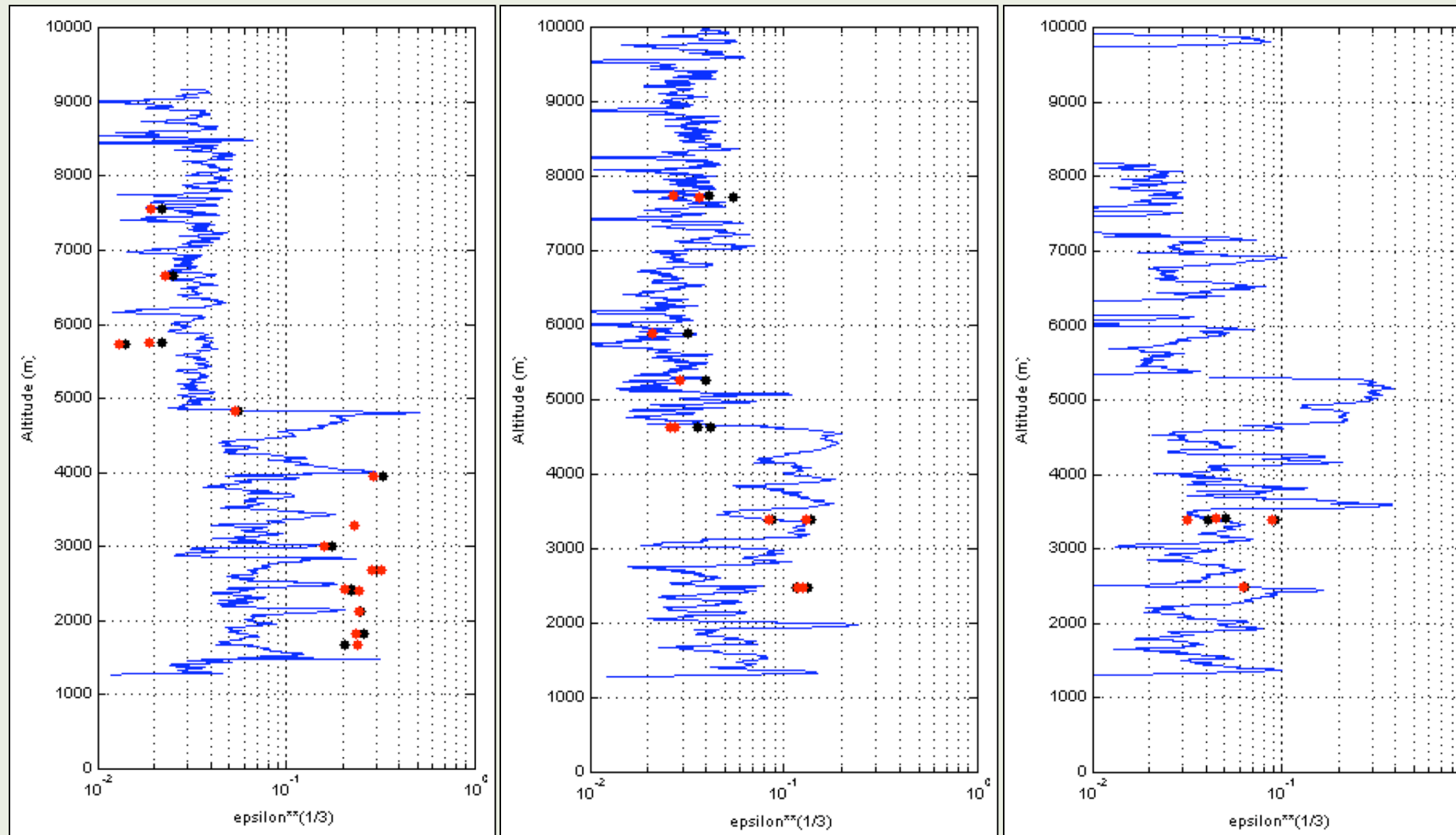


IMAGe TOY 2008 Geophysical
Turbulence Phenomena

Comparison with Aircraft Data along the Sonde Track



IOP 03 (March 09)

IOP 13 (April 16)

IOP 15 (April 26)

Black points - x component, Red points - average of 3 components

Summary

- Low-level terrain-induced perturbations consist predominantly of (partially) trapped lee waves – long wavelength waves (>30 km) have largest amplitudes
- Lower-tropospheric turbulence zones: Behind the leading edge of the wave updrafts and underneath wave crests, Turbulence levels encountered light to severe
- Internal rotor structure: KH instability of the separated BL vortex sheet leads to preponderance of small scale eddies within the rotor
- Estimates of turbulence dissipation rate (TDR) from dropsonde data utilizing stably stratified turbulence arguments agrees well with TDR derived from aircraft observations